Article

SOURCE DATA | TRANSPARENT PROCESS | OPEN ACCESS

THE EMBO JOURNAL

Clock component OsPRR73 positively regulates rice salt tolerance by modulating *OsHKT2;1*-mediated sodium homeostasis

Hua Wei[1,2], Xiling Wang[1,2], Yuqing He[1,2], Hang Xu[1,2] & Lei Wang[1,2,*]

Abstract

The roles of clock components in salt stress tolerance remain incompletely characterized in rice. Here, we show that, among *OsPRR* (*Oryza sativa Pseudo-Response Regulator*) family members, *OsPRR73* specifically confers salt tolerance in rice. Notably, the grain size and yield of *osprr73* null mutants were significantly decreased in the presence of salt stress, with accumulated higher level of reactive oxygen species and sodium ions. RNA sequencing and biochemical assays identified *OsHKT2;1*, encoding a plasma membrane-localized Na^+ transporter, as a transcriptional target of OsPRR73 in mediating salt tolerance. Correspondingly, null mutants of *OsHKT2;1* displayed an increased tolerance to salt stress. Immunoprecipitation-mass spectrometry (IP-MS) assays further identified HDAC10 as nuclear interactor of OsPRR73 and co-repressor of *OsHKT2;1*. Consistently, H3K9ac histone marks at *OsHKT2;1* promoter regions were significantly reduced in *osprr73* mutant. Together, our findings reveal that salt-induced *OsPRR73* expression confers salt tolerance by recruiting HDAC10 to transcriptionally repress *OsHKT2;1*, thus reducing cellular Na^+ accumulation. This exemplifies a new molecular link between clock components and salt stress tolerance in rice.

Keywords circadian clock; *OsPRR73*; ROS; salt stress; sodium transporter
Subject Categories Chromatin, Transcription & Genomics; Membranes & Trafficking; Plant Biology
DOI 10.15252/embj.2020105086 | Received 24 March 2020 | Revised 27 October 2020 | Accepted 13 November 2020 | Published online 21 December 2020
The EMBO Journal (2021) 40: e105086

Introduction

Salinization of the cultivated land is increasingly imposing severe constraints on plant adaptation and crop yield. Excess sodium (Na^+), the most widespread soluble cation in salinized soil, damages plants mainly by resulting in sequential osmotic stress and oxidative stress for glycophyte crops including rice (Munns & Tester, 2008; Ismail *et al*, 2014; Zhu, 2016; Yang & Guo, 2018a; Yang & Guo, 2018b). On the other hand, plants also need to uptake Na^+ as a nutrient, especially in the potassium limited conditions (Horie *et al*, 2007). Hence, to survive on the salinized soil, plants have evolved intricate mechanisms to maintain Na^+ homeostasis, which are mainly gated by ion transporters (Munns & Tester, 2008; Zhu, 2016; Yang & Guo, 2018a). It has been demonstrated that members of the High-affinity K^+ transporters (HKT) are required for maintaining Na^+ homeostasis, thus regulating salt tolerance (Oomen *et al*, 2012; An *et al*, 2017; Kobayashi *et al*, 2017).

In plants, there are two subfamilies of HKTs. Subfamily I of HKTs is conserved in both monocotyledonous and dicotyledonous species by acting as Na^+-selective transporter, including rice OsHKT1;1, OsHKT1;4, and OsHKT1;5, which mainly contribute to Na^+ exclusion upon salt stress (Wang *et al*, 2015; Suzuki *et al*, 2016; Kobayashi *et al*, 2017). By contrast, the subfamily II of HKTs, only present in monocots, includes the transporters permeable to both Na^+ and K^+, such as plasma membrane-localized OsHKT2;1 which mediates Na^+ uptake, and its mRNA expression is rapidly repressed under salt stress (Horie *et al*, 2007). Consistently, *oshkt2;1* mutants accumulate less Na^+, but not K^+ (Horie *et al*, 2007). The abundance of *OsHKT2;1* was intricately regulated at both transcriptional and post-translational levels. ETHYLENE INSENSITIVE3-LIKE1 (OsEIL1) and OsEIL2 were shown to directly activate *OsHKT2;1* expression, hence negatively regulating salt tolerance in rice seedlings (Yang *et al*, 2015). Recently, OsSIRH2-14, a (RING) H2-type E3 ligase, was found to physically interact with OsHKT2;1 protein at the high salinity condition and regulate its stability through 26S-proteosome pathway (Park *et al*, 2019). Notably, *OsHKT2;1* overexpressing lines displayed the reduced salt stress tolerance in both rice and *Arabidopsis* (Ardie *et al*, 2009), suggesting a potential role of *OsHKT2;1* in rice salt stress tolerance. Nonetheless, the molecular mechanism underlying salt-induced *OsHKT2;1* repression that results in reduced Na^+ uptake is largely unknown.

The circadian clock, the endogenous time-keeping system in higher plants, has been demonstrated to function as an important integrator of multiple abiotic stresses signals, including salt stress in *Arabidopsis* (Greenham & McClung, 2015; Sanchez & Kay, 2016). For instance, the salinity stress responsive genes are expressed rhythmically in constant light condition, suggesting that there are

1 Key Laboratory of Plant Molecular Physiology, CAS Center for Excellence in Molecular Plant Sciences, Institute of Botany, Chinese Academy of Sciences, Beijing, China
2 University of Chinese Academy of Sciences, Beijing, China
*Corresponding author. Tel: +86 10 62836165; E-mail: wanglei@ibcas.ac.cn

regulated by circadian clock (Covington *et al*, 2008). In addition, *EARLY FLOWERING 3* (*ELF3*), which mediates light input to circadian clock, is required for salt tolerance by modulating critical regulatory components in salt stress response pathways at both transcriptional and post-translational levels (Sakuraba *et al*, 2017). Moreover, salinity stress triggers protein degradation of GIGANTEA (GI), one of the major clock components, resulting in the release of SOS2 (Salt Overly Sensitive 2) sequestration to thus confer salt tolerance by subsequently activating SOS1, the major plant Na^+/H^+-antiporter (Kim *et al*, 2013). In addition, high salinity could alter core clock gene expression, including the repression of *PSEUDO-RESPONSE REGULATOR 7* (*PRR7*) and *TIMING OF CAB EXPRESSION 1* (*TOC1*), but induction of *PRR9* (Kwon *et al*, 2014). Intriguingly, the triple mutant of *prr579* was more tolerant to salt stress (Nakamichi *et al*, 2009) with unknown mechanism. Together these results indicate that the clock components PRR members may play a key role in mediating salt stress tolerance in *Arabidopsis*. In rice, it has been implicated that the expression of SOS pathway genes including *OsSOS2* and *OsSOS3* is affected by diurnal rhythm in seedling stage (Soni *et al*, 2013). In addition, a number of circadian-regulated genes were shown to be involved in salinity tolerance in rice, such as *cyclophilin 2* (*OsCYP2*) and *Receptor for Activated C Kinase 1* (*OsRACK1*) (Ruan *et al*, 2011; Zhang *et al*, 2018a). Nevertheless, whether rice core clock components participate in salt tolerance and the underlying mechanisms remain largely unclear.

The *OsPRR* (*Oryza sativa Pseudo-Response Regulator*) gene family consists of five members and is expressed with robust oscillation pattern from dawn to dusk, sequentially with approximately 2-h intervals, in the order *OsPRR73* (*OsPRR37*), *OsPRR95* (*OsPRR59*), and *OsPRR1* (Murakami *et al*, 2003). Similar to AtPRR proteins, all the OsPRR proteins contain a Pseudo-Response (PR) motif at their N terminus and a CCT (CONSTANS, CONSTANS-Like, and TOC1) domain at the C terminus, which functions as a DNA-binding motif. Ectopic expression of *OsPRRs* in the respective *Arabidopsis prr* mutants confirmed that they are in part genetically interchangeable with *AtPRRs* (Murakami *et al*, 2007). Notably, *OsPRR37* was found to be the causal gene for quantitative trait locus (QTL) of *HD2* (*Heading date* 2) and indirectly regulates grain productivity and regional adaptation, which is critical for rice breeding to achieve desired photosensitivity (Murakami *et al*, 2005; Koo *et al*, 2013; Yan *et al*, 2013; Gao *et al*, 2014). However, the role of *OsPRRs* in rice abiotic stress tolerance, especially salt stress, and the underlying mechanism remains elusive.

Here, we systematically generated the loss-of-function mutants of *OsPRRs* and found among *OsPRR* members, *OsPRR73* is the unique member required for rice salt tolerance. *OsPRR73* was rapidly induced by NaCl treatment and *oprr73* null mutants were hypersensitive to sodium ion stress. Transcriptomic and biochemical analyses further identified *OsHKT2;1* as a novel transcriptional target of OsPRR73 in mediating salt tolerance. Additionally, OsPRR73 could physically interact with the histone deacetylase 10 (HDAC10) to form a repressive complex to repress *OsHKT2;1* transcription by altering its promoter chromatin status. Consistently, null mutant of *OsHKT2;1* generated by CRISPR/Cas9 approach exhibits the enhanced salt tolerance phenotype. Together, we conclude that OsPRR73 transcriptionally represses *OsHKT2;1* upon salt stress hence to modulate sodium ions homeostasis and confer salt tolerance in rice.

Results

OsPRR73 positively regulates rice salinity stress tolerance

To examine whether circadian clock components contribute to salt tolerance in rice, we investigated the roles of rice orthologs of the *Arabidopsis Pseudo-Response Regulator* (*PRR*) gene family members in salinity response. The transcript profiles of *OsPRR1*, *OsPRR37*, *OsPRR59*, *OsPRR73,* and *OsPRR95* were first determined under salt stress. Evidently, among *OsPRR* members, *OsPRR73* showed most pronounced induction in response to 180 mM NaCl, while the transcript levels of *OsPRR1* and *OsPRR95* showed no discernible changes (Appendix Fig S1). The expression of *OsPRR73* in the roots was also induced by salt (Appendix Fig S1F) as seen in shoots (Appendix Fig S1D).

By searching a rice T-DNA insertion mutant database (Jeon *et al*, 2000), we identified an *OsPRR73* mutant 3A-12296 in Dongjin (DJ) background, in which the T-DNA was inserted into the fifth intron of *OsPRR73* (Fig 1A). Genomic PCR and RT–qPCR analyses confirmed that 3A-12296 (hereafter referred as *osprr73*) is a null mutant allele of *OsPRR73* (Fig EV1). To eliminate the unrelated traits potentially caused by additional T-DNA insertions elsewhere, we backcrossed the *osprr73* mutant with DJ and conducted subsequent physiological analysis using homozygous F3 progenies. We also generated null mutants *osprr37*, *osprr59*, and *osprr95* by using CRISPR/Cas9 technology as previously described (Ma *et al*, 2015). By using TILLING approach, we also identified an *osprr1* null mutant with a premature stop codon in *OsPRR1* which resulted in 147 aa truncated protein (Fig EV2). The salt stress tolerance phenotypes were determined by transferring 4-week-old seedlings into media containing 180 mM NaCl for 21 days, followed by recovery in regular hydroponic culture for additional 7 days unless otherwise noted. Intriguingly, only the null mutant of *OsPRR73* displayed hypersensitivity to salinity stress (Fig 1B and C) with a significant reduction of survival rate, while other *osprr* null mutants showed similar salinity sensitivity to their respective wild-type control (Fig EV3). Importantly, the genetic complementation lines of *OsPRR73* could reverse the hypersensitive phenotypes of *osprr73* mutant to salinity stress.

To further validate the role of *OsPRR73* in salinity stress tolerance, we generated three *osprr73* CRISPR/Cas9 alleles with a 33 bp deletion 184 bp downstream of ATG (*osprr73-C*1), a premature stop codon (*osprr73-C*2) caused by 5 bp deletion, and a premature stop codon (*osprr73-C*3) caused by 1 bp insertion (Fig EV2). The Cas9-free homozygous lines were subsequently used for examining salt stress tolerance phenotype. Notably, the *osprr73-C*2 and *osprr73-C*3 plants were more sensitive to salinity stress, while the *osprr73-C*1 displayed modest phenotype, indicating that *osprr73-C*1 might be a weak allele, while *osprr73-C*2 and *osprr73-C*3 were likely null alleles (Fig 1E and F). Moreover, both *osprr73* allele in DJ background and *osprr73-Cs* alleles in NIP background contained significantly lower levels of chlorophyll (Fig 1G) and much higher levels of membrane ion leakage (Fig 1H) in the presence of NaCl. In addition, the grain yield and fertility of *osprr73* mutant were dramatically reduced upon irrigation with 75 mM NaCl solution (Appendix Fig S2). Collectively, these results suggest that *OsPRR73* specifically regulates rice salinity stress tolerance by acting as a positive regulator.

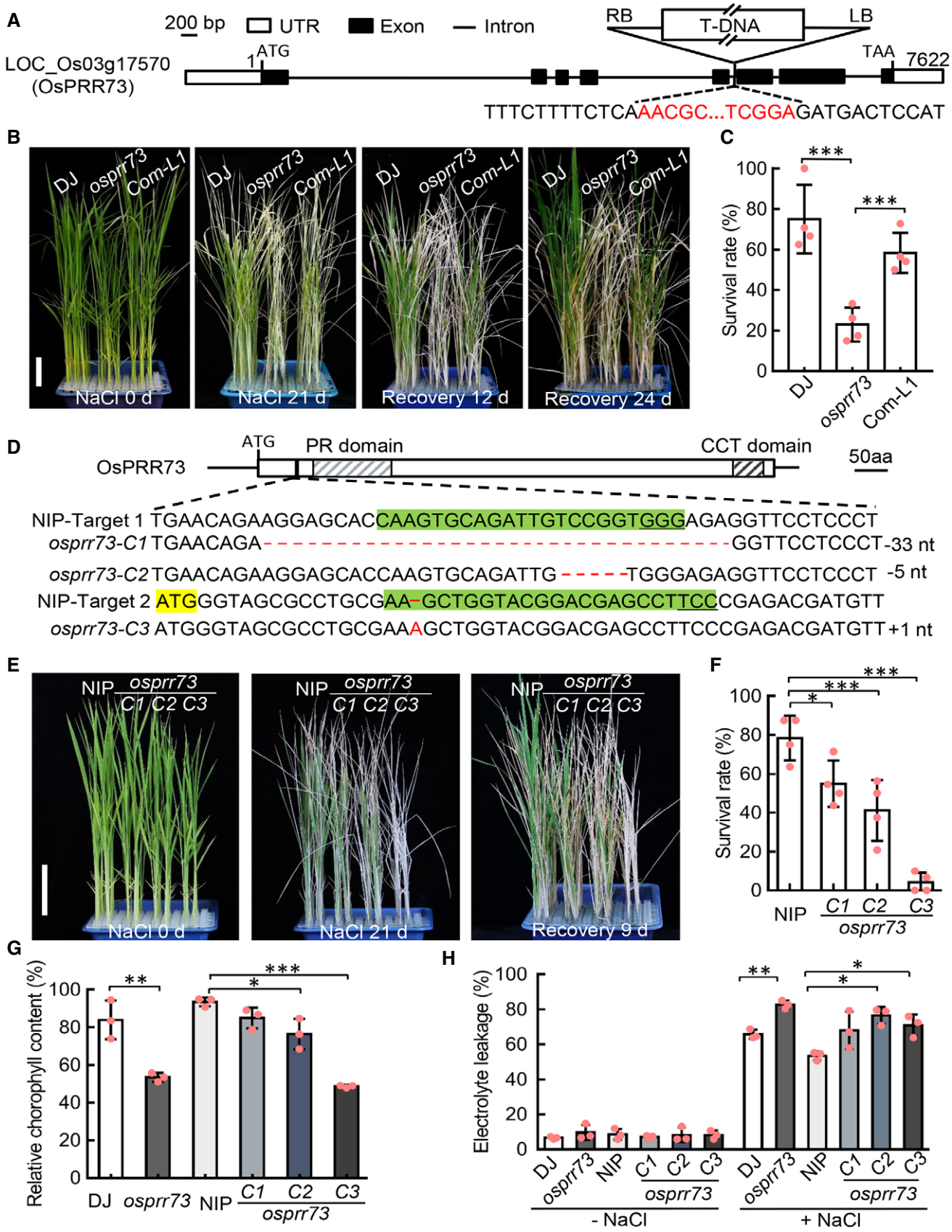
A
200 bp
UTR
Exon
Intron
RB
T-DNA
LB
LOC_Os03g17570
(OsPRR73)
ATG
TAA
7622
TTTCTTTTCTCAAACGC...TCGGAGATGACTCCAT
B
DJ
osprr73
Com-L1
NaCl 0 d
NaCl 21 d
Recovery 12 d
Recovery 24 d
C
Survival rate (%)
DJ
osprr73
Com-L1
D
OsPRR73
ATG
PR domain
CCT domain
50aa
NIP-Target 1 TGAACAGAAGGAGCACCAAGTGCAGATTGTCCGGTGGGAGAGGTTCCTCCCT
osprr73-C1 TGAACAGA----------GGTTCCTCCCT -33 nt
osprr73-C2 TGAACAGAAGGAGCACCAAGTGCAGATTG-----TGGGAGAGGTTCCTCCCT -5 nt
NIP-Target 2 ATGGGTAGCGCCTGCGAA-GCTGGTACGGACGAGCCTTCCCGAGACGATGTT
osprr73-C3 ATGGGTAGCGCCTGCGAAAGCTGGTACGGACGAGCCTTCCCGAGACGATGTT +1 nt
E
NIP
osprr73
C1 C2 C3
NaCl 0 d
NaCl 21 d
Recovery 9 d
F
Survival rate (%)
NIP
C1 C2 C3
osprr73
G
Relative chorophyll content (%)
DJ
osprr73
NIP
C1 C2 C3
osprr73
H
Electrolyte leakage (%)
DJ
osprr73
NIP
C1 C2 C3
osprr73
- NaCl
+ NaCl

Figure 1.

Figure 1. *OsPRR73* positively regulates salinity tolerance in rice.

A Schematic diagram showing the T-DNA insertion sites in rice *osprr73*$^{T\text{-}DNA}$ mutant (hereafter named as *osprr73*).

B *OsPRR73* confers salinity stress tolerance in rice. The seedlings of Dongjin (DJ, the wild-type control), *osprr73*, and the complementation line of *osprr73* (abbreviated as Com-L1) grown under 12-h light/12-h dark conditions for 28 days (left panel), transferred to 180 mM NaCl for 21 days (middle panel) and recovered for 12 and 24 days (the two right panels), respectively. Scale bar, 5 cm.

C Statistical analysis of the survival rate of DJ, *osprr73*, and Com-L1 plants in (B) after recovery 12 days. Data are presented as mean ± SD. (*n* from 4 biological replicates, and 24 plants were tested in each of biological replicates). (***) $P \leq 0.001$ were generated by Student's *t*-test.

D Diagram showing the target and mutated sites of *OsPPR73* by CRISPR/Cas9-based genome editing. The PR and CCT are the abbreviations of Pseudo-Response and COSTANS, COSTANS-LIKE, and TOC1 domains, respectively. The target sequences within the first exon of *OsPRR73* were shown with the green boxes. PAM sequences were labeled with underline within the green boxes.

E Null mutant of *osprr73* in Nipponbare (NIP) background by genome editing displayed hypersensitivity to NaCl treatment. Scale bar, 5 cm.

F Survival rate of NIP (wild type of CRISPR lines) and *osprr73-C* (*C* stands for CRISPR) plants in (E) after recovery 9 days. Data are presented as mean ± SD. $n = 4$ biological replicates, 24 plants for each biological replicate. (*) $P \leq 0.05$ and (***) $P \leq 0.001$ were generated by Student's *t*-test.

G, H Quantification of chlorophyll content and electrolyte leakage of WT and *osprr73* mutants with or without 180 mM NaCl treatment for 7 days. Data are presented as mean ± SD. n = 3, biological replicates, and asterisks represent significant difference among means by Student's *t*-test with (*) $P \leq 0.05$, (**) $P \leq 0.01$, (***) $P \leq 0.001$.

Source data are available online for this figure.

Next to investigate whether *OsPRR73* functions as a clock component in rice, we performed time course RT–qPCR analysis to examine the temporal expression patterns of circadian clock-related genes (Izawa *et al*, 2011; Nagano *et al*, 2012; Bendix *et al*, 2015; Matsuzaki *et al*, 2015) including *OsPRRs*, *OsGI*, *OsFKF1*, *OsCCA1*, *OsLHY*, *OsLUX*, *OsELF3.1*, and *OsLKP2*, in the free-running condition which is usually used for assaying circadian phenotypes (Millar *et al*, 1995; Wang & Tobin, 1998). We found that their oscillation profiles were unanimously altered in *osprr73* mutant with evident delayed peak or trough phase (Fig EV4). Moreover, we conducted time course RT–qPCR of *osprr73* plants grown in the natural photoperiodic conditions, with 2-h interval over a day–night cycle. We found the transcriptional peaks of *OsPRR1*, *OsPRR37*, and *OsLUX* genes were dramatically reduced (Appendix Fig S3A, B and J), whereas the transcriptional peaks of *OsGI* and *OsFKF1* were markedly increased in *osprr73* mutant, in relation to wild-type DJ (Appendix Fig S3F and G). Additionally, there were marginal discrepancies of the expression patterns of *OsCCA1, OsLHY, OsELF3.1,* and *OsLKP2* between *osprr73* and DJ (Appendix Fig S3H, I, K and L), suggesting that *OsPRR73* may not directly regulate these genes under this natural diurnal condition. Noticeably, the transcriptional peak of *OsGI*, previously proposed as a core clock component (Izawa *et al*, 2011), was elevated in *osprr73* plants under both free-running and natural diurnal conditions (Fig EV4F and Appendix Fig S3F). Together, these data support a notion that circadian clock was altered in *osprr73* plants, and OsPRR73 likely acts as a clock component in rice, as its ortholog in *Arabidopsis*.

Transcriptomic analysis of the *osprr73* mutant

To determine the subcellular localization of OsPRR73, we transiently expressed the *GFP-OsPRR73* fusion gene in leaves of *Nicotiana benthamiana* and found it was predominantly localized in the nuclei of epidermal cells (Appendix Fig S4A), consistent with its annotated function as a transcriptional regulator. We then reasoned that the transcriptomic analysis might provide additional insights into the role of OsPRR73 in salinity stress response. Hence, RNA-seq analysis was performed to reveal the transcriptomic profiles of *osprr73* mutant and DJ in the shoots of the 2-week-old plants treated with NaCl 4 and 28 h, respectively, as *OsPRR73* were highly expressed in shoots (Appendix Fig S4B). We set $P < 0.05$ and the value of fold change ($\log_2$) over 1.5 relative to DJ as the cutoff threshold. In total, we identified 690, 627, and 1,419 up-regulated genes and 742, 795, and 996 down-regulated genes in *osprr73* mutant compared with the DJ control of mock, 4-h, and 28-h NaCl treatment, using three biological replicates (Fig 2A). RT–qPCR results confirmed the transcript profiles of eight randomly selected differentially expressed genes (DEGs) in *osprr73* mutants (Appendix Fig S5). Venn diagram analysis revealed 1,030, 999, and 1,663 unique DEGs in *osprr73* mutant treated with mock, NaCl 4 h, and NaCl 28 h, respectively (Fig 2B). Gene Ontology (GO) analysis further revealed that the top enriched GO terms in the short-term NaCl (4 h) treatment were involved in response to stimulus (GO:0050896), response to stress (GO:0006950), and oxidation reduction (GO:0055114) (Fig 2C). By contrast, the most enriched GO terms in the long-term NaCl treatment (28 h) were the regulation of cellular metabolic process (GO:0031323), regulation of metabolic process (GO:0019222), and regulation of primary metabolic process (GO:0080090) (Appendix Fig S6). Under the mock treatment, the DEGs in *osprr73* mutant were mainly involved in response to stress and stimulus (Fig 2D). However, the most affected biological processes upon NaCl treatment were the DEGs in response to oxidative stress and oxidation reduction (Fig 2D).

Interestingly, the sodium ion transporter (GO:000681) was specifically enriched among DEGs with NaCl treatment (Fig 2D), implicating sodium ion transporters might be involved in salt stress response in *osprr73* mutant. Furthermore, eight DEGs in 4-h NaCl treated *osprr73* plants were overlapped with previously well-characterized 157 salt stress responsive genes (Fig 2E), including two sodium transporter (LOC_Os06g48810 and LOC_Os01g20160). Next, heatmap analysis with the RNA-seq data clearly demonstrated that transcript level of LOC_Os06g48810 encoding OsHKT2;1 was induced, while LOC_Os03g25500 encoding a cytochrome P450 was repressed (Fig 2F) in *osprr73* mutant with 4-h NaCl treatment. Together, these results implicate that abnormal Na^+ and ROS homeostasis might contribute to the hypersensitive salinity response in *osprr73* mutant.

OsPRR73 confers sodium ion stress response

To further investigate whether Na^+ accumulation was the direct cause for hypersensitivity of *osprr73* mutant to NaCl stress, we checked Na^+ contents in both shoots and roots in *osprr73* mutants. There was no obvious difference in Na^+ content between *osprr73*

mutant and DJ under non-NaCl stress condition (Fig 3A). However, with 180 mM NaCl treatment for 7 days, the Na^+ content was significantly higher in both shoots and roots of *osprr73* (Fig 3A). Similarly, the Na^+ content in *osprr73-C* lines of NIP background was also significantly higher (Appendix Fig S7A). Meanwhile, we measured K^+ contents with the same samples and found there was no evident difference between *osprr73* and DJ under either normal or NaCl stress condition (Fig 3B and Appendix Fig S7B). Thus, even though there was no difference or even lower in the Na^+/K^+ ratio of the plants under un-stressed condition, the Na^+/K^+ ratio was increased in *osprr73* mutant plants after 180 mM NaCl treatment (Fig 3C), which might contribute to their hypersensitivity to NaCl treatment

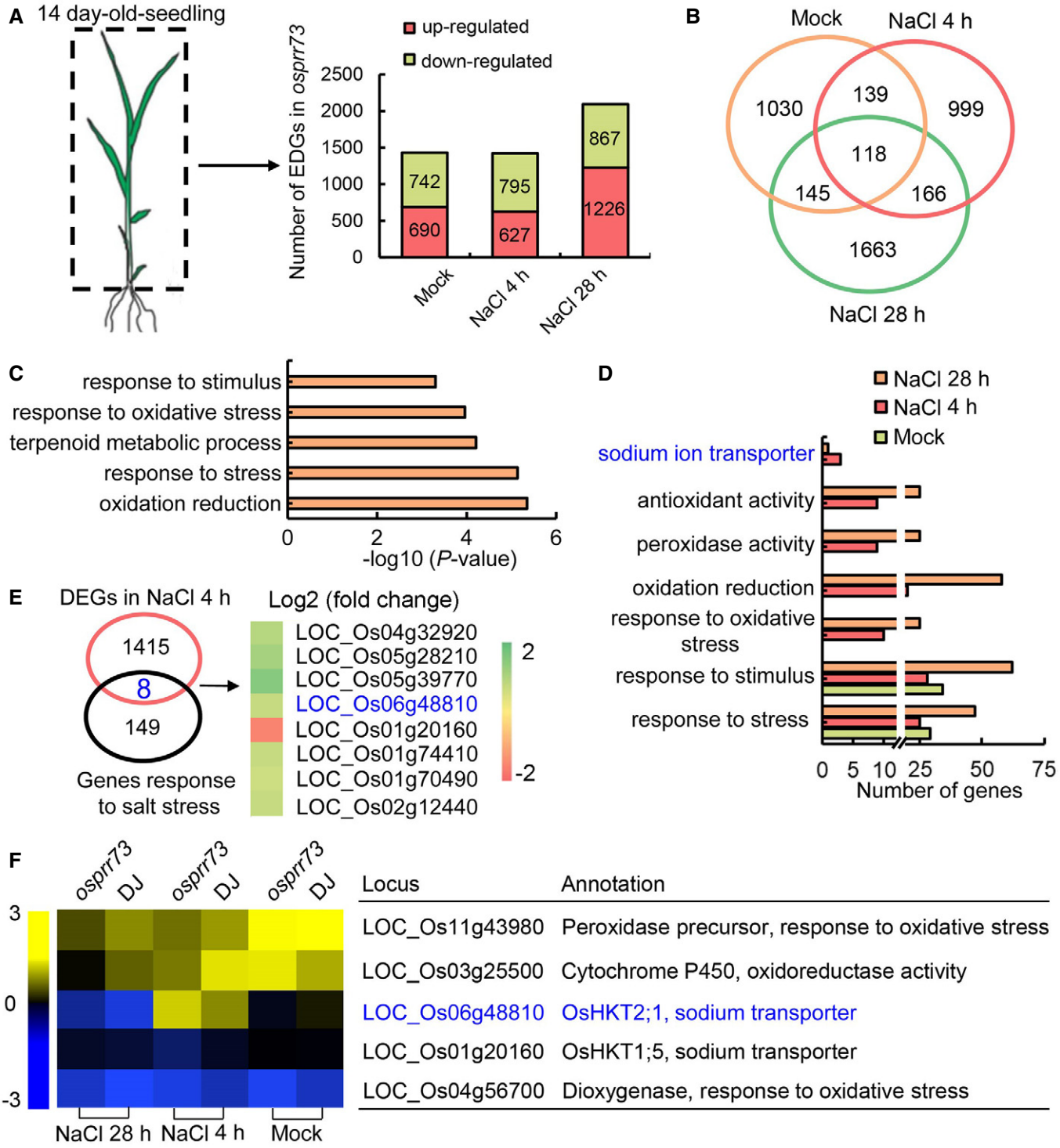

Locus	Annotation
LOC_Os11g43980	Peroxidase precursor, response to oxidative stress
LOC_Os03g25500	Cytochrome P450, oxidoreductase activity
LOC_Os06g48810	OsHKT2;1, sodium transporter
LOC_Os01g20160	OsHKT1;5, sodium transporter
LOC_Os04g56700	Dioxygenase, response to oxidative stress

Figure 2.

Figure 2. Differential expressed genes in *osprr73* mutant upon salinity stress as revealed by RNA-seq.

A Schematic diagram for tissues (left panel) and the number of differentially expressed genes (right panel) in *osprr73* mutant compared with their respective wild type (DJ).

B Venn diagram showing the number of differentially expressed genes in *osprr73* mutant with or without salinity stress.

C GO (Gene ontology) classification of differentially expressed genes in *osprr73* mutant treated by NaCl for 4 h, based on biological process (BP). *P*-values were generated by Fisher's test.

D The number of differentially expressed genes, which belongs to BP cluster in GO analysis, in *osprr73* mutant.

E Venn diagram showing the overlapped DEGs in *osprr73* mutants (pink circle) with previously identified salt-responsive genes which derived from China rice data center (black circle). Heatmap showing 6 common genes, the colored bar represents $\log_2$ (fold change).

F Heat map of *OsHKT2;1*, *OsHKT1;5*, and the genes related to the oxidative stress in GO analysis, showing their transcriptional abundance in *osprr73* mutant. The colored bar indicates log2 (FPKM) values.

(Zhu, 2016; Yang & Guo, 2018b). Together with the transcriptomic analysis results, we proposed that *OsPRR73* might play a vital role in maintaining sodium ion homeostasis to confer salt stress tolerance.

To further distinguish whether hypersensitivity in *osprr73* mutant was caused by Na^+ or Cl^- accumulation, we utilized different salt solution including Na_2SO_4, and $MgCl_2$ to treat *osprr73* mutant and DJ plants. Interestingly, the *osprr73* mutant plants displayed hypersensitivity to 90 mM Na_2SO_4 (Fig 3D and E), but not 90 mM $MgCl_2$ treatment (Fig 3F and G), suggesting that *OsPRR73* is required for Na^+-associated stress. As Na^+ accumulation subsequently produces osmotic stress, we test the osmotic stress sensitivity by treating *osprr73* mutant with 180 mM mannitol. As shown in Fig 3H and I, *osprr73* plants displayed similar osmotic stress sensitivity to DJ. Hence, we concluded that the main cause for hypersensitivity of salinity stress in *osprr73* may be due to the abnormal accumulation of Na^+.

OsHKT2;1 is a direct transcriptional target of OsPRR73

Since the *osprr73* mutant is specifically sensitive to Na^+ stress with abnormally high cellular Na^+ accumulation, and transcript abundance of *OsHKT2;1* was up-regulated in *osprr73* mutant, we were promoted to determine whether *OsHKT2;1* is a direct transcriptional target of *OsPRR73*. Intriguingly, we found *OsHKT2;1* displayed a robust oscillation pattern with an acrophase in the morning and trough level at evening (Appendix Fig S8), which was overall an antiphase with the temporal expression profile of *OsPRR73* (Appendix Fig S8G and H). Next, we assessed the transcript levels of *OsHKT2;1* in *osprr73* mutant by RT–qPCR and found its levels were significantly higher in *osprr73* mutant, especially with either short-term (4 and 16 h) or long-term (72 h) 180 mM NaCl treatment (Fig 4A). In addition, we detected the diurnal expression pattern of *OsHKT2;1* in *osprr73* and WT plants with or without NaCl stress presence. We found that the transcript levels of *OsHKT2;1* are significantly higher in *osprr73* mutant especially in the presence of salt stress (Appendix Fig S9), suggesting *OsPRR73* can efficiently repress the expression of *OsHKT2;1* upon salt treatment. We also determined the transcript levels of *OsHKT1;5*, encoding a Na^+ exporter, and found its transcript level was only modestly altered in the short-term NaCl treatment (Fig 4B). Together, these results implied that *OsHKT2;1*, but not *OsHKT1;5*, was a potential target of OsPRR73.

To further determine whether *OsHKT2;1* was a direct target of OsPRR73, we employed a transient co-expression assay using *N. benthamiana* leaf infiltration. Evidently, OsPRR73 could significantly repress the transcriptional activity of *OsHKT2;1* promoter (Fig 4C and D). As *Arabidopsis* ortholog of OsPRR73 mainly binds G-box containing sequence, we performed *cis*-element scanning within the ~ 1.5 Kb promoter region of *OsHKT2;1* using PlantCARE database (Lescot *et al*, 2002) and found there were two potential G-box elements at −456 bp (S3) and −1,298 bp (S4) upstream of start codon (Fig 4E). Chromatin immunoprecipitation (ChIP) assay using *35S:GFP-OsPRR73* transgenic lines grown in 12-h light/12-h dark for 2 weeks and samples collected at ZT12. The two amplicons containing a potential G-box element (S3 and S4) were significantly enriched (Fig 4E) in ChIP-qPCR assay. In contrast, there were no significant enrichments for other regions and a negative control in selected ubiquitin promoter (Fig 4E). We then used electrophoresis mobility shift assay (EMSA) to determine whether OsPRR73 could directly bind the enriched region using OsPRR73-CCT, the DNA-binding domain, tagged by myelin basic protein (MBP). As shown in Fig 4F, a specific shifted band was observed when the labeled DNA probes, which contains an atypical G-box element (CACGAC), were incubated with MBP-OsPRR73-CCT. No band shift was observed in the presence of non-labeled or mutated G-box probe, implicating that OsPRR73 could directly bind the promoter of *OsHKT2;1*. Together, our data support the notion that *OsHKT2;1* is a direct transcriptional target of OsPRR73.

OsPRR73 directly interacts with rice histone deacetylase HDAC10

To further explore the mechanism by which OsPRR73 repressed *OsHKT2;1* transcriptionally, we revealed the interactome of OsPRR73 through immunoprecipitation followed by mass spectrometry (IP-MS). Two-week-old seedlings of T2 progeny of *35S: GFP-OsPRR73* transgenic line in DJ background were used for IP-MS as previously described (Wang *et al*, 2019). In total, we identified 19 nuclear proteins in OsPRR73 complex shared by two biological replicates (Appendix Table S1). Among them, SDG704 (LOC_Os11g38900), encoding a SET-domain containing protein, and Histone Deacetylase 10 (HDAC10, LOC_Os12g08220) were potential components related to transcriptional suppression. Since SDG704 was unable to methylate H3K9 (Ding *et al*, 2007), we determined whether HDAC10 were a *bona fide* interactor of OsPRR73.

Using transient co-expression of GFP-OsPRR73 and HDAC10-FLAG proteins in *N. benthamiana* leaves, we observed strong co-immunoprecipitation of HDAC10 with GFP-OsPRR73 (Fig 5A). A split-luciferase imaging analysis confirmed the interaction between OsPRR73 and HDAC10 *in vivo* (Fig 5B). Moreover, bimolecular-fluorescence complementation (BiFC) analysis revealed positive signal in the nucleus of leave epidermal cells when YFP^N-OsPRR73 and YFP^C-HDAC10 were co-expressed (Fig 5C). We also found that the truncated OsPRR73 containing PR (PSEUDO-RESPONSE) domain and without CCT (CONSTANS, CONSTANS-like, and TOC1) domain

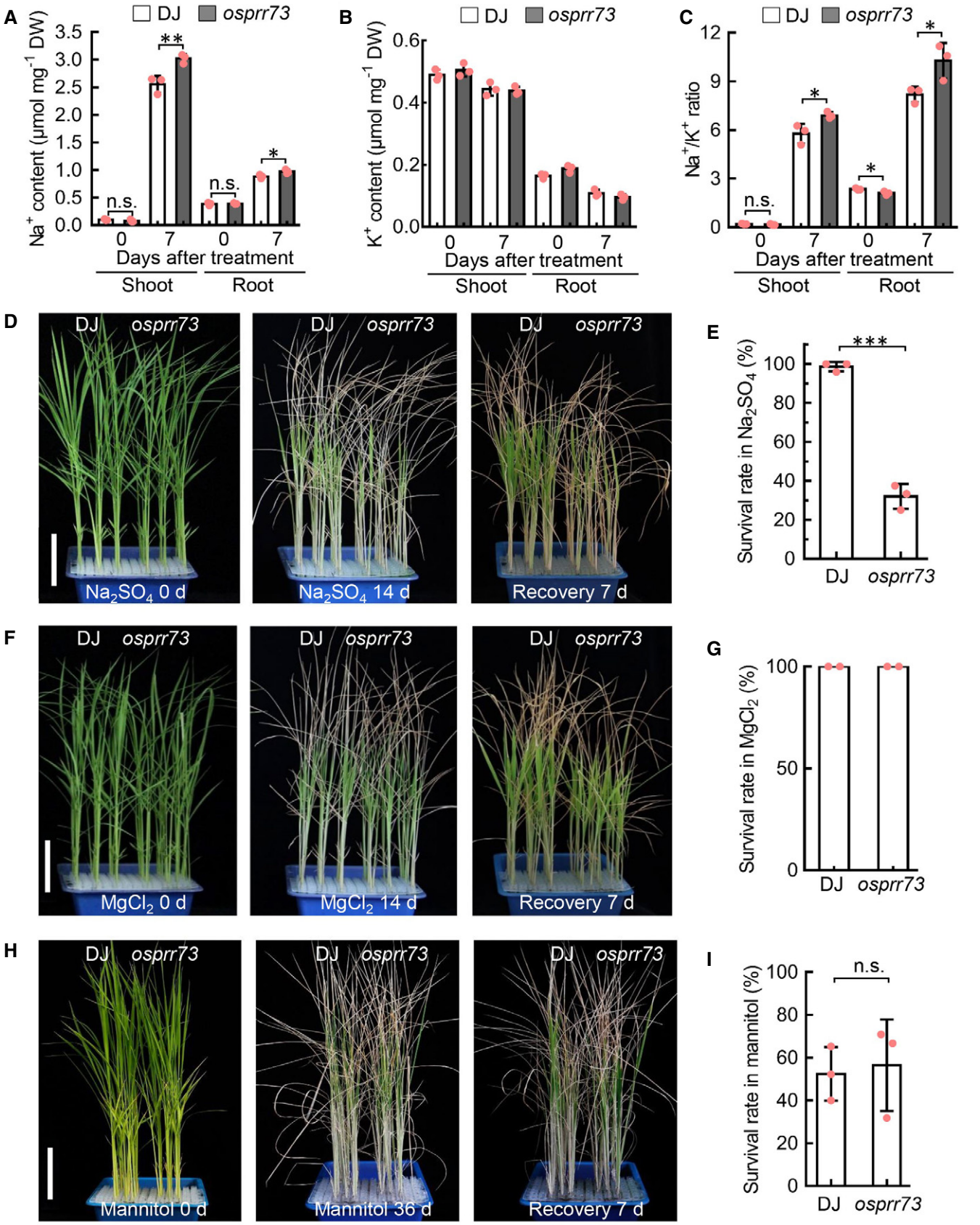
A
DJ
osprr73
Na+ content (μmol mg-1 DW)
3.5
3.0
2.5
2.0
1.5
1.0
0.5
0.0
**
*
n.s.
n.s.
0
7
0
7
Days after treatment
Shoot
Root
B
DJ
osprr73
K+ content (μmol mg-1 DW)
0.6
0.4
0.2
0.0
0
7
0
7
Days after treatment
Shoot
Root
C
DJ
osprr73
Na+/K+ ratio
12
9
6
3
0
*
*
*
n.s.
0
7
0
7
Days after treatment
Shoot
Root
D
DJ
osprr73
Na2SO4 0 d
Na2SO4 14 d
Recovery 7 d
E
***
Survival rate in Na2SO4 (%)
100
80
60
40
20
0
DJ
osprr73
F
DJ
osprr73
MgCl2 0 d
MgCl2 14 d
Recovery 7 d
G
Survival rate in MgCl2 (%)
100
50
0
DJ
osprr73
H
DJ
osprr73
Mannitol 0 d
Mannitol 36 d
Recovery 7 d
I
n.s.
Survival rate in mannitol (%)
100
80
60
40
20
0
DJ
osprr73

Figure 3.

Figure 3. The *osprr73* mutant displays specific hypersensitivity to sodium ion stress.

A, B The Na^+ and K^+ contents in the shoots and roots of DJ and *osprr73* mutant plants with or without 180 mM NaCl treatment for 7 days. Na^+ (A) and K^+ (B) contents were measured with ICP method. Data represent means ± SD, (n = 3, biological replicates). (**) $P \leq 0.001$ and (*) $P \leq 0.001$ indicate significant difference by Student's t-test. The abbreviation of n.s. stands for no significant.

C Ratio of Na^+ to K^+ was calculated with their respective content in (A) and (B). Data represent mean ± SD (n = 3, biological replicates). For each of biological replicates, 6 individual plants were measured. The asterisk represents significant difference among means by Student's t-test with (*) $P \leq 0.05$, and n.s. indicates no significant.

D Four-week-old seedlings of DJ and *osprr73* were treated with 90 mM Na_2SO_4 for 14 days (middle panel) and recovered for additional 7 days (right panel). Scale bar, 5 cm.

E Statistical analysis of survival rates with Na_2SO_4 treatment in (D). Data represent means ± SD. n = 3 biological replicates, 24 plants for each biological replicate. (***) $P \leq 0.001$ indicates significant difference by Student's t-test.

F The seedlings of DJ and *osprr73* mutant were treated with 90 mM $MgCl_2$ for 14 days (middle panel) and recovered for 7 days (right panel). Scale bar, 5 cm.

G Statistical analysis of survival rates with $MgCl_2$ treatment in (F). The survival rate of DJ and *osprr73* plants in $MgCl_2$ stress were calculated after recovery 7 days. Data represent means ± SD. n = 2 biological replicates, 24 plants of each replicate.

H The seedlings of DJ and *osprr73* mutant were treated with 180 mM mannitol for 36 days (middle panel) and recovered for 7 days (right panel). Scale bar, 5 cm.

I The survival rate of DJ and *osprr73* plants in mannitol stress. Data represent means ± SD. n = 3 biological replicates, 24 plants of each replicate. The abbreviation of n.s. stands for no significant generated by Student's t-test.

Source data are available online for this figure.

(1–711 amino acids, OsPRR73-F1) was capable of interacting with HDAC10. Deletion of both PR and CCT domain (200–711 amino acids, OsPRR73-F2) almost abolished the interaction with HDAC10 (Fig 5D), suggesting that the N-terminal PR domain of OsPRR73 was required for interacting with HDAC10. To determine whether the interaction between OsPRR73 and HDAC10 could affect the level of H3ac on the promoter of *OsHKT2;1*, we further performed ChIP-qPCR assay with H3K9ac antibody. We found that the levels of H3K9ac on the promoter regions of S3 and S4 were significantly increased in *osprr73* mutant compared with DJ (Fig 5E), while H3 levels were about the same between *osprr73* mutant and DJ (Fig 5F), indicating that the interaction between OsPRR73 and HDAC10 could affect H3ac. To further examine the regulatory role of HDAC10 on *OsHKT2;1*, we conducted a transient co-expression assay using *N. benthamiana* leaf infiltration. As expected, HDAC10 could modestly repress the transcriptional activity of *OsHKT2;1*. Noticeably, the repressive effect of OsPRR73 on *OsHKT2;1* transcription was augmented by co-transforming with HDAC10, indicating that the interaction between OsPRR73 and HDAC10 can inhibit the transcription of *OsHKT2;1* more efficiently (Appendix Fig S10A and B). Together, our results suggested that OsPRR73 might recruit the histone decatylase HDAC10 to repress the transcription of *OsHKT2;1*.

OsHKT2;1 negatively regulates rice salinity tolerance

Previously, *OsHKT2;1* was shown to be responsible for Na^+ uptake in K^+ starved rice plants (Horie *et al*, 2007) and had an impact on potassium use efficiency (Hartley *et al*, 2020). However, the role of *OsHKT2;*1 in salinity stress tolerance is unclear. As *OsHKT2;1* is a direct transcriptional target of OsPRR73 (Fig 4), and higher level of Na^+ was accumulated in *osprr73* mutant plants (Fig 3A), we hypothesized that increased transcript level of *OsHKT2;1* in *osprr73* caused the higher Na^+ accumulation, which might result in salinity hypersensitivity phenotype of *osprr73* mutant. Hence, we were promoted to investigate whether *OsHKT2;1* was required for rice salinity stress tolerance. By employing CRISPR/Cas9 technology, we generated the *oshkt2;1* mutant in NIP background. Sanger sequencing confirmed that the first exon of *OsHKT2;1* had 1 base pair insertion in *oshkt2;1* mutant (Fig 6A and B), resulted in a premature stop codon (Fig 6C). The Cas9-free homozygous seedlings of F3 progeny were used for examining salinity stress tolerance phenotype. Before NaCl treatment, the morphology of *oshkt2;1* was indistinguishable compared with NIP plants; however, after salinity stress, the survival rate of *oshkt2;1* was higher than that of NIP (Fig 6D and E), suggesting *OsHKT2;1* was indeed involved into salinity stress tolerance.

Figure 4. OsPRR73 binds *OsHKT2;1* promoter to repress its transcription.

A, B The expression level of *OsHKT2;1* and *OsHKT1;5* in *osprr73* mutant and the wild control Dongjin (DJ) plants with or without salinity stress in multiple time points. DJ Data represent means ± SD. n = 3, technical replicates. The representative data are from at least two individual biological replicates. The asterisks represent significant difference among means by Student's t-test with (*) $P \leq 0.05$, (**) $P \leq 0.01$ and (***) $P \leq 0.001$.

C Transient expression assay in the infiltrated leaves of *Nicotiana benthamiana* showing OsPRR73 can repress *OsHKT2;1* transcription. Left panel showing the bioluminescence signal of OsHKT2;1 and OsPRR73. Bioluminescence of co-transformation of either GFP or *35S: GFP-OsPRR73* (GFP-OsPRR73) with *OsHKT2;1pro: LUC* in *N. benthamiana*.

D Quantification of bioluminescence intensity of *OsHKT2;1pro: LUC* shown in (C). Data represent means ± SD. n = 10. The asterisks indicate the significant difference by Student's t-test with (***) $P \leq 0.001$. At least two biological replicates were conducted with similar results.

E ChIP-qPCR assay showing the enriched DNA fragments including the S3 and S4 regions of *OsHKT2;1* promoter by OsPRR73, compared with wild-type DJ controls. The amplicon of *Ubiquitin* was taken as a negative control. Two-week-old seedlings were harvested at ZT12. Data represent means ± SD (n = 3, technical repeats). The experiments were performed at least two biological replicates with similar result. Top scheme indicates the locations of amplicons for ChIP analysis. The asterisks represent significant difference among means by Student's t-test with (**) $P \leq 0.01$.

F EMSA assay with the OsPRR73 incubated with the probes designed for the S4 region of *OsHKT2;1* promoter. Unlabeled probes were used as competitor with indicated folds. MBP alone was used as negative control. Arrowhead marks the shifted positive bands.

Source data are available online for this figure.

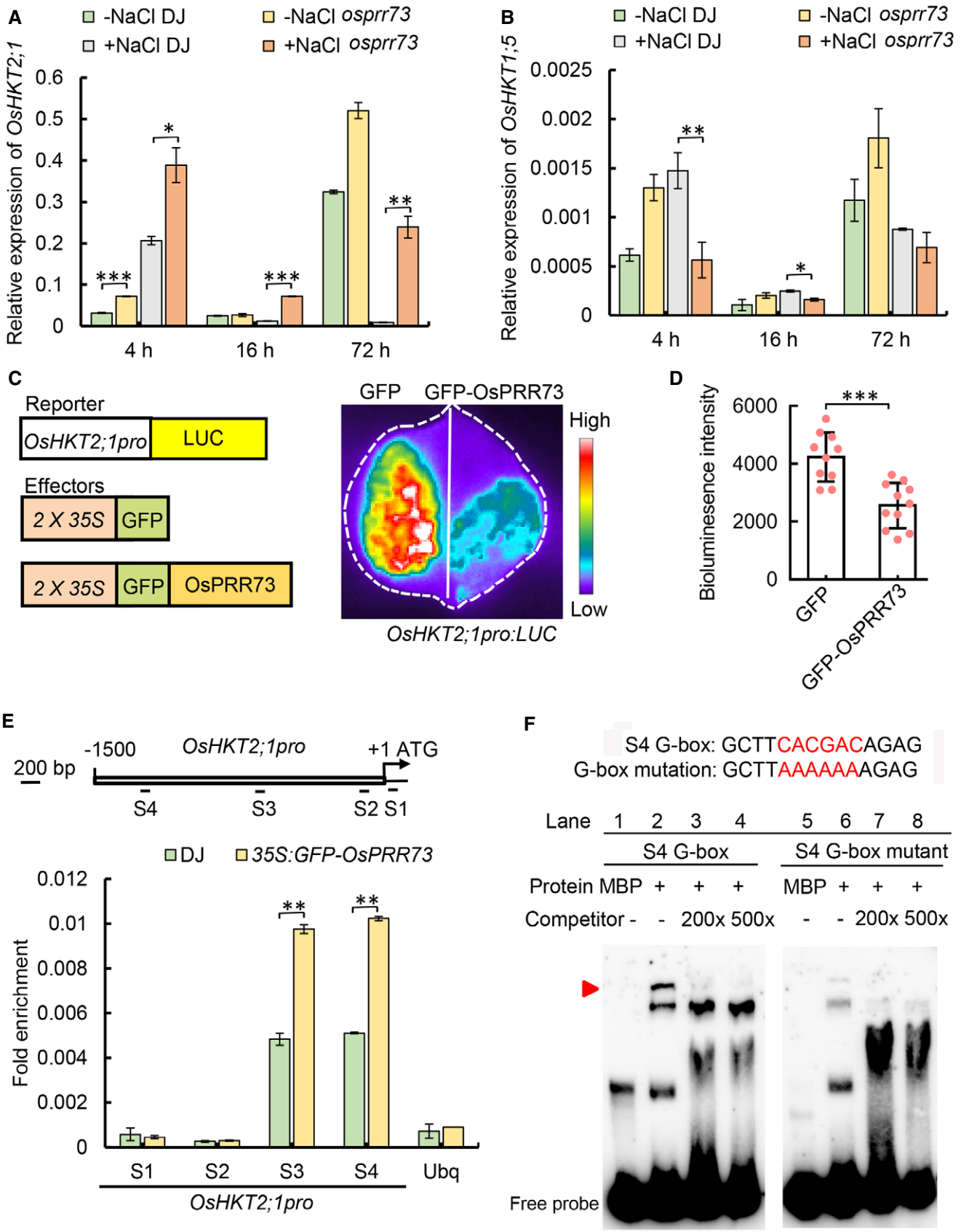
A
-NaCl DJ
+NaCl DJ
-NaCl osprr73
+NaCl osprr73
Relative expression of OsHKT2;1
0.6
0.5
0.4
0.3
0.2
0.1
0
***
*
***
**
4 h
16 h
72 h
B
-NaCl DJ
+NaCl DJ
-NaCl osprr73
+NaCl osprr73
Relative expression of OsHKT1;5
0.0025
0.002
0.0015
0.001
0.0005
0
**
*
4 h
16 h
72 h
C
Reporter
OsHKT2;1pro
LUC
Effectors
2 X 35S
GFP
2 X 35S
GFP
OsPRR73
GFP
GFP-OsPRR73
High
Low
OsHKT2;1pro:LUC
D
Bioluminesence intensity
6000
4000
2000
0
***
GFP
GFP-OsPRR73
E
200 bp
-1500
OsHKT2;1pro
+1 ATG
S4
S3
S2 S1
DJ
35S:GFP-OsPRR73
Fold enrichment
0.012
0.01
0.008
0.006
0.004
0.002
0
**
**
S1
S2
S3
S4
Ubq
OsHKT2;1pro
F
S4 G-box: GCTTCACGACAGAG
G-box mutation: GCTTAAAAAAAGAG
Lane 1 2 3 4 5 6 7 8
S4 G-box
S4 G-box mutant
Protein MBP + + + MBP + + +
Competitor - - 200x 500x - - 200x 500x
Free probe

Figure 4.

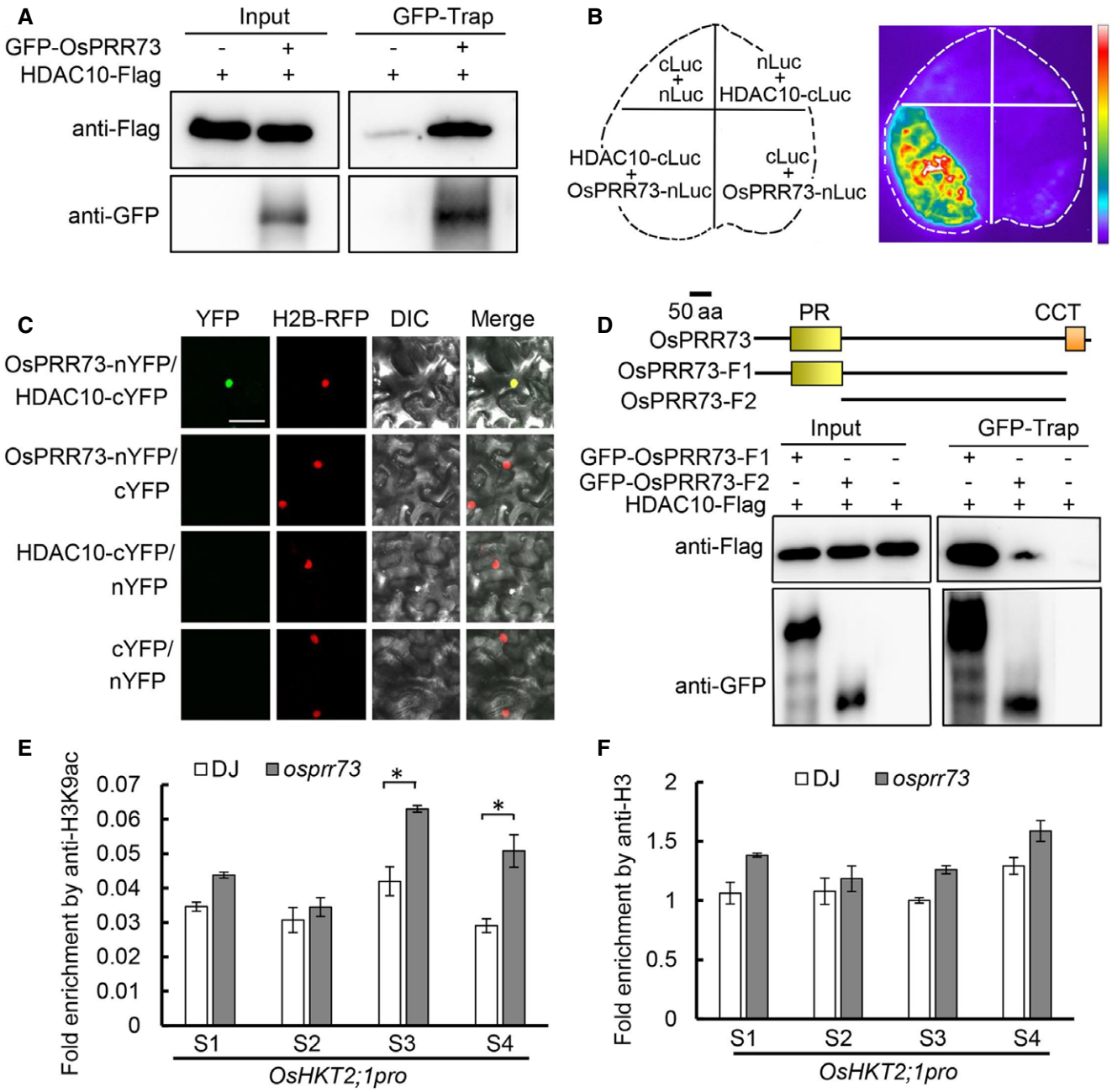

Figure 5. OsPRR73 physically interacts with HDAC10 in nucleus.

A Co-immunoprecipitation assay showing the physical interaction between OsPRR73 and HDAC10 *in vivo*. CoIP was conducted with GFP-Trap beads, and GFP and FLAG antibodies were used to detect OsPRR73 and HDAC10 in immunoprecipitants as indicated.

B Split-luciferase complementation (SLC) assay showing OsPRR73 interacts with HDAC10 in the co-infiltrated *N. benthamiana* leaves.

C Bimolecular-fluorescence complementation (BiFC) assay shows the interaction between OsPRR73 and HDAC10 occurs in nucleus. BF represents bright field. Scale bar, 40 μm.

D N terminus of OsPRR73 containing PR domain is required and sufficient for interacting with HDAC10. Upper panel shows the schematic illustration of full-length and the truncated OsPRR73 proteins. CoIP was performed with GFP-Trap beads, and immunoprecipitants were detected by FLAG for HADC10 and GFP for truncated proteins of OsPRR73, respectively.

E, F Chromatin Immunoprecipitation-qPCR (ChIP-qPCR) assay to detect the enriched promoter regions of OsHKT2;1 by using the H3K9ac (E) and H3 (F) antibodies. Two-week-old seedlings were harvested at ZT12. The locations of amplicons were described in Fig 4E. Data represent means ± SD. $n = 3$ technical replicates. The asterisk indicates the significant difference by Student's *t*-test with (*) $P \leq 0.05$. The experiments were repeated at least twice with similar result.

Source data are available online for this figure.

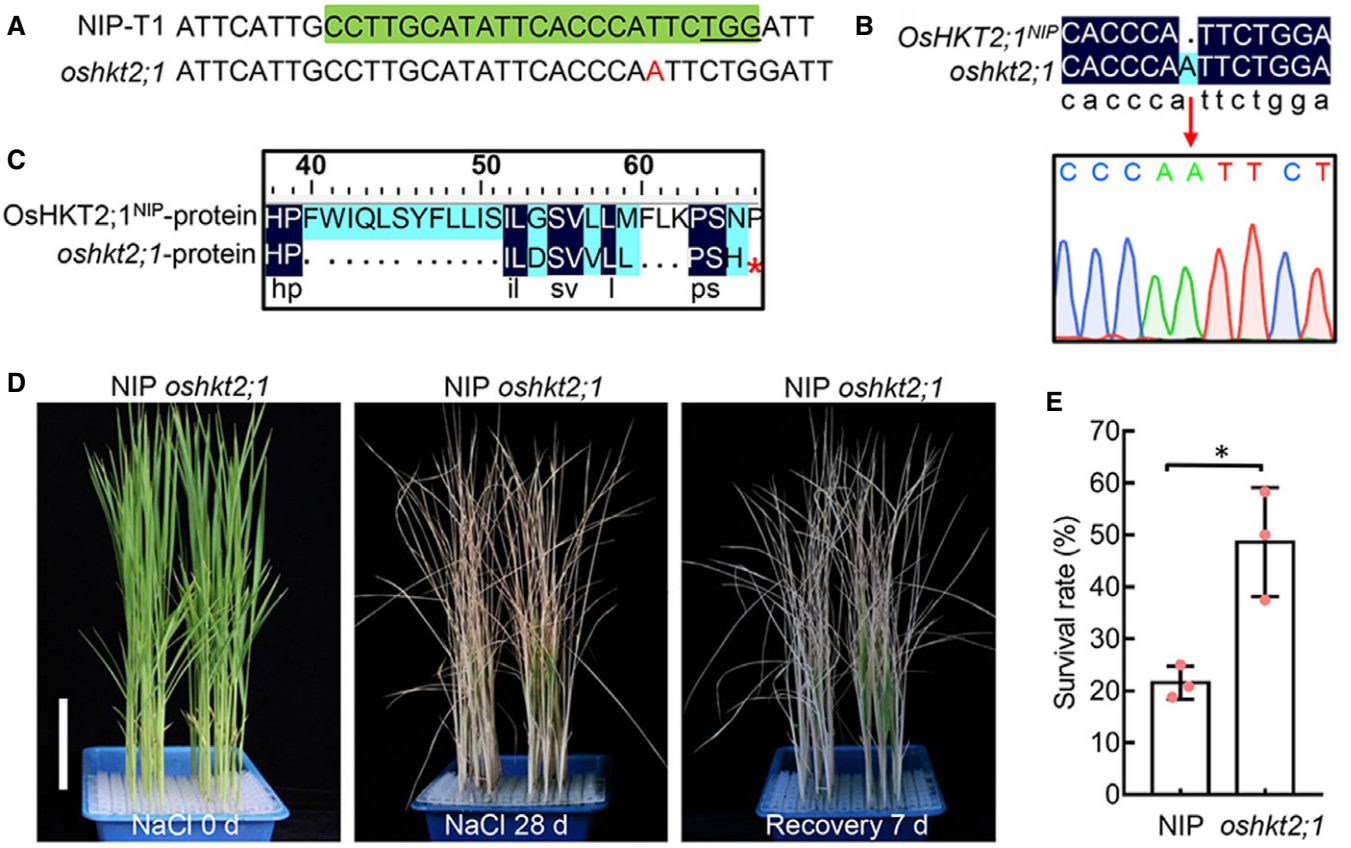

Figure 6. *OsHKT2;1* negatively regulates salinity tolerance in rice.

A Nucleotide sequence showing the mutated site of *OsHKT2;1* generated via CRISPR/Cas9-based genome editing. Green box indicates the CRISPR target sequence, which locates on the first exon of *OsHKT2;1*. PAM sequences were labeled with underline within the green boxes.

B Sanger sequencing confirmed the *oshkt2;1* mutant harbor a 1-bp insertion (pointed by red arrowheads).

C Alignment the amino acid sequences of OsHKT2;1, and its mutated version showing a premature stop codon occurred in the ORF of *OsHKT2;1*.

D The *oshkt2;1* seedling is more tolerant to the treatment of NaCl. The *oshkt2;1* and NIP, its wild-type, 4-week-old seedlings grown under NaCl conditions for 0 days (left panel), then were transferred to 200 mM NaCl for 28 days (middle panel), and recovered for 7 days (right panel). Scale bar, 5 cm.

E Statistical analysis of survival rate in (D). Data represent means ± SD. $n = 3$ biological replicates, 24 plants of each replicate. (*) $P \leq 0.05$ was generated by Student's *t*-test.

Source data are available online for this figure.

OsPRR73 may indirectly inhibit the accumulation of reactive oxygen species

ROS accumulation is considered as a secondary response of salt stress. High ROS contents in plant cells can damage proteins, lipids, and other cellular components (Yang & Guo, 2018a). Our RNA-seq data showed that the genes related to oxidative stress were enriched in GO analysis; we thus explored if ROS was abnormally acumulated in *osprr73* mutant upon salt stress. We measured the malondialdehyde (MDA) contents, an indicator of membrane lipid peroxidation (Ouyang *et al*, 2010), and found its level in *osprr73* mutant was very similar to DJ under normal condition. However, upon NaCl treatment, MDA content was dramatically increased in *osprr73* mutant, much higher than that in DJ plants (Fig 7A). In addition, diaminobenzidine (DAB) staining and 2′, 7′-dichlorodihydrofluorescein diacetate (H_2DCFDA) fluorescent signal also confirmed the high ROS contents in shoots and roots of *osprr73* mutant only under salinity stress (Fig 7B–D). Similar results were obtained in *osprr73* null mutant generated by CRISPR/Cas9 (Appendix Fig S11A and B) in NIP background. Consistently, the ROS-scavenging enzyme activities of superoxide dismutase (SOD; EC 1.15.1.1) and catalase (CAT, EC1.11.1.6) were significantly reduced in *osprr73* mutants under salinity stress condition (Fig 7E and F, and Appendix Fig S11C and D). Taken together, *OsPRR73* appeared to negatively regulate accumulation of ROS caused by salinity stress. Finally, application of H_2O_2 did not affect the expression of *OsPRR73* under either short or long time treatment (Appendix Fig S12A and B), which implicated that OsPRR73 might affect the oxidative stress response indirectly. In addition, we also detected the accumulation of ROS in *oshkt2;1* mutant with both DAB staining and H_2DCFDA fluorescent signal as an indicator. We found that the ROS content was significantly reduced in both leaves and roots of *oshkt2;1* mutant in the presence of NaCl stress (Appendix Fig S13), indicating *OsHKT2;1* may negatively regulate ROS accumulation in response to salt stress.

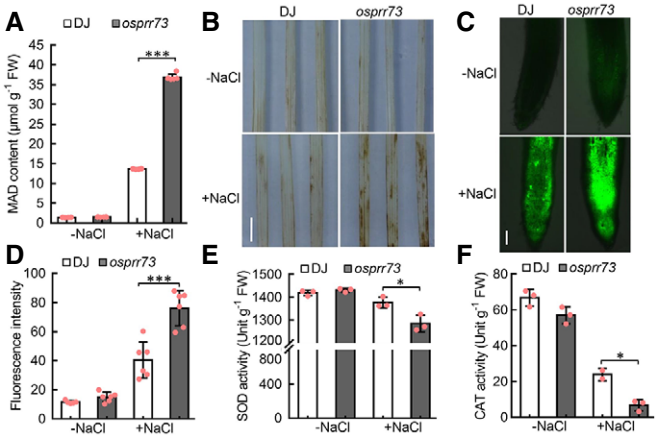

Figure 7. ROS was highly accumulated in *osprr73* mutant under salinity stress.

A Malondialdehyde (MDA) content in leaves of 14-day-old DJ and *osprr73* plants treated by 180 mM NaCl for 3 d and normal condition. Data represent means ± SD. $n = 6$, biological replicates. The asterisks indicate the significant difference (***) $P \leq 0.001$ by student's *t*-test.

B DAB staining showing the greater ROS accumulation in the leaves of *osprr73* mutant treated by 180 mM NaCl treatment for 3 days. Scale bar, 1 cm.

C H_2O_2 concentration was detected by using H_2DCFDA in the root tip of DJ and *osprr73* mutant plants. Scale bar, 5 mm. −NaCl and +NaCl represented the untreated or treated plants by NaCl, respectively.

D Quantitative analysis of H_2O_2 concentration in the root of DJ and *osprr73* mutant. Data represent means ± SD. $n \geq 6$. The asterisks indicate the significant difference (***) $P \leq 0.001$ by Student's *t*-test.

E, F Measurement of SOD (Superoxide dismutase) (E) and CAT (Catalase) (F) enzymes activity in shoots of DJ and *osprr73* seedlings with or without NaCl stress. Data represent means ± SD. $n = 3$ technical replicates. Data are representative from two independent biological replicates with similar result. The asterisks indicate the significant difference (*) $P \leq 0.05$ by Student's *t*-test.

Source data are available online for this figure.

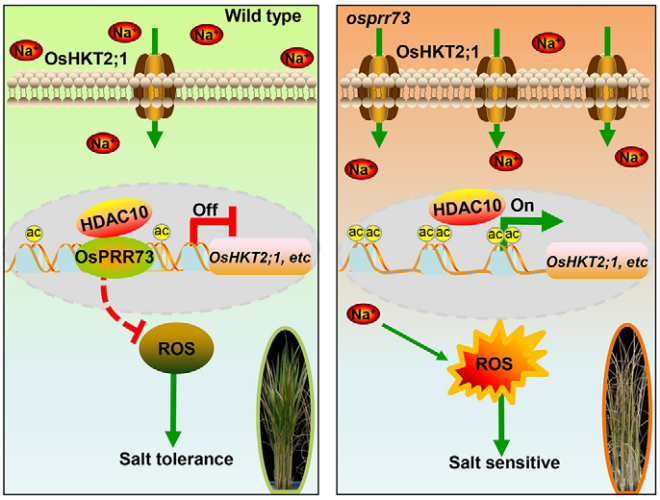

Figure 8. Proposed working model for *OsPRR73* conferred salinity tolerance in rice.

OsPRR73 binds the promoter of *OsHKT2;1*, by recruiting HDAC10, to negatively regulate the expression of *OsHKT2;1* to reduce the import of cellular sodium ion, which subsequently reduced ROS accumulation, thus conferring salinity stress (left panel). In the absence of *OsPRR73*, the transcription inhibition of *OsHKT2;1* was released, hence resulted in sodium ion accumulation. The excessive sodium ion subsequently accumulation caused ROS accumulation, to forming a Na^+-ROS stress cascade, leading to decreased survival.

Discussion

It has been implicated that clock components could be involved in the regulation of salinity stress tolerance in *Arabidopsis* (Nakamichi *et al*, 2009; Kim *et al*, 2013). Meanwhile, circadian clock was shown to act as a crucial regulator to enhance fitness under unfavorable conditions, by providing temporal regulatory mechanisms for the sessile organisms (Sanchez & Kay, 2016). However, whether rice clock component contributes to salt tolerance remains unclear yet. Here, we found that the null mutants of *OsPRR73* generated either by T-DNA insertion or CRISPR/Cas9 approach, displayed hypersensitive to salt stress, which could be detrimental to rice grain yield. We further revealed the underlying molecular mechanism, which was in part due to the de-repression of *OsHKT2;1* that subsequently caused enhanced Na^+ uptake followed by secondary ROS accumulation. Moreover, we found that HDAC10 could physically interact with OsPRR73 to form a transcriptional repression complex to inhibit *OsHKT2;1* expression. Consistently, the null mutant of *OsHKT2;1* was more tolerant to salt stress. Moreover, the *oshkt2;1 osprr73* double mutant also displayed the salt-tolerant phenotype with much less ROS accumulation, similar to that of *oshkt2;1* plant (Fig EV5), suggesting that *OsHKT2;1* is a major downstream component to mediate the salt hypersensitivity of *osprr73* plants. Our findings thus revealed an *OsPRR73-OsHKT2;1* molecular module that confers the salt tolerance in rice via regulating Na^+ homeostasis (Fig 8), which represents a novel molecular link between circadian clock and salt tolerance in rice.

The expression pattern of *OsPRR73* was previously shown to be quite similar to that of *OsPRR37* in both diurnal and constant light condition (Murakami *et al*, 2003). Here, we found that *OsPRR73*, but not *OsPRR37*, was specifically required for salt stress tolerance. Previous findings demonstrated that *OsPRR37* was a major factor to determine rice heading time in the long day condition (Murakami *et al*, 2005; Koo *et al*, 2013; Yan *et al*, 2013; Gao *et al*, 2014), suggesting that despite *OsPRR73* and *OsPRR37* share similar temporal expression pattern, their physiological functions are distinct. Our time course RT–qPCR assay with plants grown in both free-running and natural diurnal conditions suggested that *OsPRR73* is involved into the regulation of circadian clock. In *Arabidopsis*, PRR proteins had been shown to form heterodimers either with other PRRs or with key regulators of plant growth and development such as CONSTANS protein (Wang *et al*, 2010; Hayama *et al*, 2017). Interestingly, we also identified OsPRR59 as an interacting protein of OsPRR73 in our IP-MS assay (Appendix Table S1), suggesting that rice OsPRR proteins likely form heterodimer as well. Hence, it will be fascinating to completely decipher the underlying mechanisms of *OsPRR73* in regulating rice circadian clock in the future, at both transcript and post-translational levels. Nonetheless, our findings collectively provide a molecular link between circadian clock and salt tolerance in rice, through regulating sodium homeostasis, which

paved a way for further deciphering regulatory network of rice circadian clock-regulated abiotic stress response.

It has been long known that OsHKT2;1 can uptake Na^+, but is rapidly repressed by salt stress (Horie *et al*, 2007), thus to maintain Na^+ homeostasis. However, the molecular mechanism for salt stress-induced repression of *OsHKT2;1* remains unknown. In our study, we found that *OsPRR73* could be rapidly induced by 4-h NaCl treatment. Meanwhile, the transcript level of *OsHKT2;1* was also induced by 4-h NaCl treatment, but was severely reduced in 8-h NaCl treated wild-type plants, which was 4 h lagged behind the peak expression of *OsPRR73*, suggesting that the transcriptional repression role of OsPRR73 might be subjected to post-transcriptional regulation. In *Arabidopsis*, the peaks of PRRs protein levels are usually delayed 2–3 h relative to their respective transcript peaks, and PRR proteins could be modified at post-translational level (Fujiwara *et al*, 2008; Wang *et al*, 2010). It would be imperative to determine the mechanisms underlying OsPRR protein peaks lagging behind their transcript peaks in the future. The mechanism for rapid induction of *OsPRR73* by NaCl treatment also remains to be elucidated. Importantly, the *OsHKT2;1* transcript level was constantly higher in *osprr73* mutant, especially in the presence of salt stress (Fig 4A), consistent with *OsHKT2;1* is a transcriptional target of OsPRR73. In addition, *OsHKT2;1* transcript level was slightly higher in the absence of NaCl treatment in *osprr73* mutant, while it was much higher upon salt treatment, suggesting that there might be other unidentified factors responsible for the acute induction of *OsHKT2;1* at the early stage of NaCl treatment.

The molecular mechanisms by which circadian clock regulates abiotic stresses, including cold and drought stress, have been extensively documented. However, the detailed mechanisms for the roles of core clock components in salt stress response are unclear, especially in rice and other monocot crops. Among the Na^+ transporters, HKT has been shown to play critical roles in both monocots and dicots in the salinity stress tolerance, via maintaining Na^+ and K^+ homeostasis (Horie *et al*, 2009; Almeida *et al*, 2013). Unlike in *Arabidopsis*, there is only one HKT gene (Uozumi *et al*, 2000); rice HKT gene family contains nine members. Among them, OsHKT1;1 and OsHKT2;4 are high-affinity potassium transporters. In this study, K^+ content was not significantly changed; instead, Na^+ was excessively accumulated in *osprr73* mutants, indicating that OsPRR73 is majorly involved in regulating Na^+ homeostasis. Besides *OsHKT2;1*, we found that transcript levels of *OsHKT1;5*, *OsHKT2;3*, and *OsNHX2* also displayed robust rhythmic patterns (Appendix Fig S8). Nevertheless, *OsHKT1;5* was only marginally decreased in *osprr73* mutant after NaCl treated 4 h and maintained at relatively similar levels to the wild-type plants, suggesting that it was unlikely a direct target of OsPRR73. *NHX2* encodes a putative Na^+/H^+ exchanger which presumably transports Na^+ from cytoplasm to vacuole to reduce cellular Na^+ toxicity (Drozdowicz & Rea, 2001). The transcript level *OsNHX2* was not significantly altered in our RNA-seq data, suggesting other core clock components might be responsible for shaping their temporal transcription pattern. Hence, as plant circadian clocks frequently integrate multiple mechanisms to regulate a crucial physiological process, it is imaginable that OsPRR73 positively regulated salt tolerance may through both directly repressing *OsHKT2;1* transcription and indirectly regulating the transcriptional abundance of other transporters, which jointly confers rice salt tolerance. Further efforts to comprehensively uncovering additional underlying pathways and identifying the superior haplotypes will surely be beneficial for breeding the salt-tolerant rice cultivars.

Materials and Methods

Plant materials and growth condition

The T-DNA insertion rice mutant of *osprr73* (3A_12296) and its wild-type Dongjin (DJ) were obtained from RiceGE (Rice Functional, http://signal.salk.edu/cgi-bin/RiceGE) and identified by the *OsPRR73*-specific primers and T-DNA right board primers which were listed in the Appendix Table S2. Then, the mutant plants were backcrossed with DJ, and the F3 homozygous progeny was used for consequent research. For obtaining *OsPRR73pro: GFP-OsPRR73* transgenic plant in DJ background, the fragment of *OsPRR73* promoter (−1,665 to −1 bp, upstream of the start codon) was firstly subcloned into *EcoR* I and *Kpn* I sites of p1300 promoterless vector, then the *OsPRR73* fragment was inserted into *Xba* I and *Pst* I sites. To make *35S: OsPRR73* constructs, the fragment of *GFP-OsPRR73* was inserted into the *Eco*RI and *Xho*I sites of the *pENTR2B* vector and then was subcloned into *35S: GFP* vector via LR recombination. All the primers used are listed in Appendix Table S2. *OsPRR73* mutants in Nipponbare (NIP) were generated with CRISPR (Clustered Regularly Interspaced Short Palindromic Repeats)/Cas9 technology according to previously described method (Ma *et al*, 2015). Briefly, the single-guide RNAs (sgRNAs) were designed to target the first exon or crucial domain of OsPRR73 and other family members to generate allelic mutants (see Appendix Table S2 for a list of sgRNAs). Then, the sgRNAs were cloned into the pYLCRISPR/$Cas9P_{ubi}$-MH vector (Ma *et al*, 2015). These constructs were transformed into *Agrobacteria tumefaciens EHA105* for inoculation with rice callus as previously reported (Hiei *et al*, 1994). To generate *OsPRR73pro: GFP-OsPRR73 osprr73* complemented plants, *osprr73* plants were crossed with the transgenic plant *OsPRR73pro: GFP-OsPRR73*. To make *oshkt2;1 osprr73* double mutant, *osprr73* plant was crossed with *oshkt2;1*. The seeds from self-pollinated and F3 homozygous plants after genotyping were used in this study.

For physiological analysis, seeds were immersed in water at 37°C for 2 days; then, the germinated seeds were placed into the bottomless 96-wells plate that containing liquid Yoshida's solution. For seedling stage of NaCl or other chemicals treatment, 4-week-old seedlings were transferred to the Yoshida's nutrient solution containing 180 mM NaCl for growing 21 days. Subsequently, they were moved to normal Yoshida's nutrient solution for recovery. After 7 days or alternative duration as noted, the survival rate was calculated according to the percentage of alive seedlings. For mature stage of NaCl treatment, the plants were grown in trays filled with soil and irrigated with 75 mM NaCl in water. Unless the specifically described, all the rice seedlings were growing under 12-h light/12-h dark, 30 ± 2°C conditions.

Measurements of the chlorophyll contention and membrane ion leakage

Measurement of total chlorophyll content was performed as described previously with minor modification (Sakuraba *et al*, 2014;

Qi *et al*, 2015; Zhang *et al*, 2018b). Briefly, the leaves of 14-day-old seedlings treated with or without 180 mM NaCl for 7 days were used for the measurement of chlorophyll content. The weight of detached leaves was recorded as fresh weight. For chlorophyll extraction, the leaves were firstly incubated in 80% acetone (*v*/*v*) in the darkness for 48 h at room temperature, and the volume was correspondingly recorded as V for calculation as the below formula. Absorbance was measured at OD645 and OD663 nm with a spectrophotometer. The chlorophyll contents were calculated according to the formula (8.02 A663 + 20.21 A645)×V/W.

The relative membrane ion leakage was measured according to the method described previously (Cao *et al*, 2007; Zhang *et al*, 2018b). In brief, seven leaves of each treatment were incubated in deionized water with gentle shaking overnight. The conductivity was measured before (C1) and after boiling for 15 min (C2) with an electro-conductivity meter. The ratio of C1:C2 represents the membrane ion leakage rate.

Determination of Na^+ and K^+ concentration

The relative ion accumulation of Na^+ and K^+ was measured according to the method described previously (Liu *et al*, 2017) with slight modification. Roots and shoots of seedlings grown in the presence or absence of NaCl treatment were separately harvested and dried before weighed. All the samples were digested with nitric acid overnight and then heated to 200°C about 8 h. All samples were diluted with MilliQ water and filtrated. The Na^+ and K^+ contents in solutions were detected by inductively coupled plasma optical emission spectrometer (ICAP6300).

Determination of the malondialdehyde

Malondialdehyde (MDA) content was determined as previously described (Zhou *et al*, 2018). Briefly, about 0.1 g of rice leaves were homogenized in 3 ml of 10% trichloroacetic acid (TCA) and centrifuged at 1,503 *g* for 10 min. Two milliliters of the supernatant were reacted with 2 ml of 0.6% (*w*/*v*) thiobarbituric acid (TBA) (made in 10% TCA). The mixture was then boiled for 15 min and centrifuged at 13,523 *g* for 10 min. The absorbance of the supernatant was read at OD450, OD532, and OD600 nm. The MDA content was estimated using the extinction coefficient of (nmol/l/cm) and expressed as μmol/g FW.

Detection of reactive oxygen species and root H_2O_2 production

The formation of hydrogen peroxide was detected by 3,3-diaminobenzidine (DAB) staining, as described before (Qiao *et al*, 2010). In brief, rice leaves from triplicate biological replicates of the samples were first cut into sections and then immersed in 10 ml staining solution with 1 mg/ml DAB containing 10 mM MES (pH 6.5). The incubation was conducted in room temperature in the dark overnight and shaking at 100 rpm. The reactions were stopped by transfer to 90% ethanol at boiling water bath until the chlorophyll was completed removed. The H_2O_2 production in roots of wild types and *osprr73* mutations under normal and NaCl stress were detected using H_2DCFDA (Molecular Probes, Thermo Fisher Scientific) based on the protocol described previously (Huang *et al*, 2009).

Measurement of peroxidase, superoxide dismutase, and catalase enzyme activity

Approx. 0.1 g rice leaves were ground with a cold mortar and pestle in 10 mM potassium phosphate buffer (pH 7.2). The homogenate was centrifuged at 1,503 *g* for 10 min at 4°C. The supernatant was crude enzyme extraction. The superoxide dismutase (SOD) and catalase (CAT) were measured using the manufacturer's protocol (Nanjing Jiancheng Bioengineering Institute) followed the instruction.

Subcellular localization observation

To detect the subcellular localization of OsPRR73, the coding sequence of *OsPRR73* was amplified and subcloned into pMDC45-GFP vector, where GFP sequence was fused to *OsPRR73* at its N terminus. The Agrobacteria harboring the corresponding construct and H2B-mCherry were co-infiltrated into the leaves of *N. benthamiana*. After 3 days, the fluorescence signals were observed by using confocal laser scanning microscope (Olympus FV 1000).

RNA-sequencing analysis

For RNA-sequencing experiments, plants were grown under 12-h light/12-h dark conditions at 30 ± 2°C for 14 days. The shoots of seedlings were harvested at the expression peak of OsPRR73 under NaCl condition 0, 4, and 28 h; the materials were frozen immediately in liquid nitrogen. The shoots from at least three seedlings were pooled to form one biological replicate, and three biological replicates were generated for each sample. RNA was extracted using a TRIzol reagent (Invitrogen). Sequencing libraries were generated using NEB Next UltraTM RNA Library Prep Kit for Illumina (NEB, USA) following manufacturer's recommendations, and index codes were added to attribute sequences to each sample. The library preparations were sequenced on an Illumina Hiseq X Ten platform and paired-end reads were generated. The RNA-seq clean reads mapped to the rice genome (MSU_v7.0) using TopHat (v2.1.1). DEseq (v1.10.1) was applied for differential gene expression analysis. Genes with $q \leq 0.05$ and $|\log_2\_ratio| \geq 1.5$ were identified as DEGs. The GO enrichment of DEGs was performed by agriGO V2.0 (http://systemsbiology.cau.edu.cn/agriGOv2/).

RT–qPCR assay

The penultimate leaf blades of 14-day-old seedlings were harvested every 3 h during a 24-h period from WT and *osprr73* plants, respectively, under continuous light to examine the expression pattern of *OsHKT2;1* and *OsPRR73*. To measure the transcript levels of *OsPRR73* under NaCl stress, the 14-day-old seedlings were treated with 180 mM NaCl, and then, the shoots and roots were sampled at every 4 h starting from treatment. Total RNA was isolated using the TRIzol reagent (Invitrogen) and reverse-transcribed into the first-strand cDNA with a PrimeScript® RT Reagent Kit (Takara). Real-time PCR was performed in an optical 96-well plate with an Applied Biosystems StepOne™ Real-Time PCR system. Each reaction contained 7.5 μl of 2 × SYBR Green Master Mix reagent, 3 μl of cDNA samples that was diluted 10-folds, and 0.3 μl of 10 μM gene-specific primers in a final volume

of 15 μl. The following PCR program was used: 95°C for 2 min, followed by 40 cycles of 95°C for 15 s, 55°C for 15 s, and 72°C for 15 s, followed by a melting-curve program. Gene expression was normalized with the transcript level of *Ubiquitin*. Two-week-old seedlings were treated with 180 mM NaCl to examine the gene expression levels under salt stress.

Transcriptional activity assay

For transcriptional activity assay, the method was described previously (Zhang *et al*, 2018b), *Agrobacterium tumefaciens AGL* carrying the fusion expression vectors effector and reporter (effector: *GFP-OsPRR73* or *GFP*; reporter: *OsHKT2;1pro:LUC-1300*) were co-transformed into the leaves of *N. benthamiana*. The luciferase signal was detected using a CCD camera at 3rd day after infiltration. The bioluminescence intensity of LUC signals was quantified by Metamorph software.

ChIP (Chromatin immunoprecipitation)-PCR

ChIP assay was performed based on the previous report (Lu *et al*, 2013) with 2-week-old *GFP-OsPRR73* transgenic seedlings, in which a mGFP coding sequence was fused in frame to the 5′-terminal of the *OsPRR73* gene in transgenic line, and the expression is driven by CaMV35S promoter. WT was used it as negative control to erase the background noise, as it did not contain GFP. The leaves of 2-week-old seedlings grown in normal nutrient solution were harvested and were cross-linked with 1% (*v*/*v*) formaldehyde under vacuum for 30 min and then ground with a cold mortar to extract the nuclear proteins for immunoprecipitation by using GFP-Trap® magnetic agarose (ChromoTek, Germany). The ChIPed DNA fragments were then used for quantitative PCR.

EMSA

The EMSA assay was conducted with Thermo Fisher kit according to the protocol described previously (Lu *et al*, 2013). The labeled probes (0.5 μl of each) were incubated with purified proteins (5 μg fusion protein per reaction) in 20-μl mixtures at 4°C for 1 h. After adding 2 μl of loading buffer, samples were loaded to electrophoresis with 0.5 × TBE buffer at 4°C for 1 h. Labeled probe and the shifted DNA–protein complexes were visualized by chemiluminescence apparatus (Tanon-5200).

Immunoprecipitation-mass spectrometry (IP-MS) assay

Two-week-old rice transgenetic seedlings of *35S:GFP-OsPRR73* grown under 12-h light/12-h dark, 30 ± 2°C conditions were collected at ZT12 (*Zeitgeber time* 12). Then, 3 ml of liquid nitrogen ground tissue powders of this sample was extracted protein and performed according to the method described previously (Wang *et al*, 2019), with two biological replicates.

Biomolecular fluorescence complementation assay

Agrobacteria containing *35S:OsPRR73-nYFP*$_{(1–158)}$ and *35S:HDAC10-cYFP*$_{(159–238)}$ were co-infiltrated into *N. benthamiana*. Agrobacteria containing H2B-mcherry was used as a nuclear marker. After 3 days, the confocal laser scanning microscope (Olympus FV1000) was used to observe the fluorescent signal of epidermal cells.

Co-immunoprecipitation assays

The coding sequence of *OsPRR73* and *HDAC10* separately were, respectively, fused to the downstream of the N-GFP or upstream of C-Flag tags. Then, the agrobactria containing *35S:GFP-OsPRR73* or *35S:HDAC10-FLAG* were co-infiltrated into leaves of *N. benthamiana*. After 3 days, the materials were harvested and ground into power in liquid nitrogen. The protein extraction and co-immunoprecipitation assays were conducted according to the method described previously with GFP-Trap beads (ChromoTek) (Wang *et al*, 2013). GFP-tagged OsPRR73, its deletions and FLAG tagged HDAC10 were detected by Western blotting using GFP antibody (ab6556, Abcam) or FLAG antibody (M2008, Abmart) as noted.

Split-luciferase assay (Split-LUC)

The coding sequence of *OsPRR73* was subcloned into the *pCAMBIA1300-nLUC* vector with *Kpn* I and *Sal* I sites, while the ORF of *HDAC10* was subcloned into *pCAMBIA1300-cLUC* vector. Then, pairwise constructs were transiently co-infiltrated into *N. benthamiana* leaves. After 3 days, the leaves were briefly immersed into the luciferin buffer for 1 min and then the LUC signals were detected by the chemiluminescence apparatus (Tanon-5200).

Accession number

Sequence data from this article can be found in the Rice Genome Annotation Project Database (http://rice.plantbiology.msu.edu/) under the following the accession numbers: *OsPRR1* LOC_Os02g40510; *OsPRR37* LOC_Os07g49460; *OsPRR59* LOC_Os11g05930; *OsPRR73* LOC_Os03g17570; *OsPRR95* LOC_Os09g36220; LOC_Os03g17560; LOC_Os03g17580; *OsHKT2;1* LOC_Os06g48810; *OsHK1;5* LOC_Os01g20160; *HDAC10* LOC_Os12g08220; *SDG704* LOC_Os11g38900; *OsCCA1* LOC_Os08g0157600; *OsLHY* LOC_Os06g0728700; *OsGI* LOC_Os01g0182600; *OsFKF1* LOC_Os11g0547000; *OsLUX* LOC_Os01g0971800; *OsELF3.1* LOC_Os06g0142600; *OsLKP2* LOC_Os02g0150800.

Data availability

The RNA-seq raw data have been deposited in NCBI SRA database with Bioproject number PRJNA602982 (https://www.ncbi.nlm.nih.gov/bioproject/PRJNA602982).

Expanded View for this article is available online.

Acknowledgements

We thank Prof. JC Jang (Ohio State University) for his constructive comments on the manuscript, and Dr. Zhuang Lu and Jingquan Li from Plant Science Facility of the Institute of Botany, Chinese Academy of Sciences for their excellent technical assistance on mass spectrometry and confocal microscopy, respectively. This work was supported by the National Key Research and Development Program of China (2016YFD0100604), National Natural Science Foundation of China (No. 31770287), and

Strategic Priority Research Program of the Chinese Academy of Sciences, Grant No. XDB27030206.

Author contributions

Research design: HW and LW; Research: HW, XW, YH, and HX; Data analysis and discussion: HW, XW, YH, HX, and LW; Manuscript writing: HW and LW.

Conflict of interest

The authors declare that they have no conflict of interest.

References

Almeida P, Katschnig D, de Boer AH (2013) HKT transporters–state of the art. *Int J Mol Sci* 14: 20359 – 20385

An D, Chen JG, Gao YQ, Li X, Chao ZF, Chen ZR, Li QQ, Han ML, Wang YL, Wang YF *et al* (2017) AtHKT1 drives adaptation of *Arabidopsis thaliana* to salinity by reducing floral sodium content. *PLoS Genet* 13: e1007086

Ardie SW, Xie L, Takahashi R, Liu S, Takano T (2009) Cloning of a high-affinity K^+ transporter gene PutHKT2;1 from puccinellia tenuiflora and its functional comparison with OsHKT2;1 from rice in yeast and *Arabidopsis*. *J Exp Bot* 60: 3491 – 3502

Bendix C, Marshall CM, Harmon FG (2015) Circadian clock genes universally control key agricultural traits. *Mol Plant* 8: 1135 – 1152

Cao WH, Liu J, He XJ, Mu RL, Zhou HL, Chen SY, Zhang JS (2007) Modulation of ethylene responses affects plant salt-stress responses. *Plant Physiol* 143: 707 – 719

Covington MF, Maloof JN, Straume M, Kay SA, Harmer SL (2008) Global transcriptome analysis reveals circadian regulation of key pathways in plant growth and development. *Genome Biol* 9: R130

Ding B, Zhu Y, Gao J, Yu Y, Cao K, Shen WH, Dong A (2007) Molecular characterization of three rice SET-domain proteins. *Plant Sci* 172: 1072 – 1078

Drozdowicz YM, Rea PA (2001) Vacuolar H^+ pyrophosphatases: from the evolutionary backwaters into the mainstream. *Trends Plant Sci* 6: 206 – 211

Fujiwara S, Wang L, Han L, Suh SS, Salome PA, McClung CR, Somers DE (2008) Post-translational regulation of the *Arabidopsis* circadian clock through selective proteolysis and phosphorylation of pseudo-response regulator proteins. *J Biol Chem* 283: 23073 – 23083

Gao H, Jin M, Zheng XM, Chen J, Yuan D, Xin Y, Wang M, Huang D, Zhang Z, Zhou K *et al* (2014) Days to heading 7, a major quantitative locus determining photoperiod sensitivity and regional adaptation in rice. *Proc Natl Acad Sci USA* 111: 16337 – 16342

Greenham K, McClung CR (2015) Integrating circadian dynamics with physiological processes in plants. *Nat Rev Genet* 16: 598 – 610

Hartley TN, Thomas AS, Maathuis FJM (2020) A role for the OsHKT2;1 sodium transporter in potassium use efficiency in rice. *J Exp Bot* 71: 699 – 706

Hayama R, Sarid-Krebs L, Richter R, Fernandez V, Jang S, Coupland G (2017) PSEUDO RESPONSE REGULATORs stabilize CONSTANS protein to promote flowering in response to day length. *EMBO J* 36: 904 – 918

Hiei Y, Ohta S, Komari T, Kumashiro T (1994) Efficient transformation of rice (*Oryza sativa* L.) mediated by agrobacterium and sequence-analysis of the boundaries of the T-DNA. *Plant J* 6: 271 – 282

Horie T, Costa A, Kim TH, Han MJ, Horie R, Leung HY, Miyao A, Hirochika H, An G, Schroeder JI (2007) Rice OsHKT2;1 transporter mediates large Na^+ influx component into K^+-starved roots for growth. *EMBO J* 26: 3003 – 3014

Horie T, Hauser F, Schroeder JI (2009) HKT transporter-mediated salinity resistance mechanisms in *Arabidopsis* and monocot crop plants. *Trends Plant Sci* 14: 660 – 668

Huang XY, Chao DY, Gao JP, Zhu MZ, Shi M, Lin HX (2009) A previously unknown zinc finger protein, DST, regulates drought and salt tolerance in rice via stomatal aperture control. *Genes Dev* 23: 1805 – 1817

Ismail A, Takeda S, Nick P (2014) Life and death under salt stress: same players, different timing? *J Exp Bot* 65: 2963 – 2979

Izawa T, Mihara M, Suzuki Y, Gupta M, Itoh H, Nagano AJ, Motoyama R, Sawada Y, Yano M, Hirai MY *et al* (2011) Os-GIGANTEA confers robust diurnal rhythms on the global transcriptome of rice in the field. *Plant Cell* 23: 1741 – 1755

Jeon JS, Lee S, Jung KH, Jun SH, Jeong DH, Lee J, Kim C, Jang S, Yang K, Nam J *et al* (2000) T-DNA insertional mutagenesis for functional genomics in rice. *Plant J* 22: 561 – 570

Kim WY, Ali Z, Park HJ, Park SJ, Cha JY, Perez-Hormaeche J, Quintero FJ, Shin G, Kim MR, Qiang Z *et al* (2013) Release of SOS2 kinase from sequestration with GIGANTEA determines salt tolerance in *Arabidopsis*. *Nat Commun* 4: 1352

Kobayashi NI, Yamaji N, Yamamoto H, Okubo K, Ueno H, Costa A, Tanoi K, Matsumura H, Fujii-Kashino M, Horiuchi T *et al* (2017) OsHKT1;5 mediates Na^+ exclusion in the vasculature to protect leaf blades and reproductive tissues from salt toxicity in rice. *Plant J* 91: 657 – 670

Koo BH, Yoo SC, Park JW, Kwon CT, Lee BD, An G, Zhang Z, Li J, Li Z, Paek NC (2013) Natural variation in OsPRR37 regulates heading date and contributes to rice cultivation at a wide range of latitudes. *Mol Plant* 6: 1877 – 1888

Kwon YJ, Park MJ, Kim SG, Baldwin IT, Park CM (2014) Alternative splicing and nonsense-mediated decay of circadian clock genes under environmental stress conditions in *Arabidopsis*. *BMC Plant Biol* 14: 136

Lescot M, Dehais P, Thijs G, Marchal K, Moreau Y, Van de Peer Y, Rouze P, Rombauts S (2002) PlantCARE, a database of plant cis-acting regulatory elements and a portal to tools for in silico analysis of promoter sequences. *Nucleic Acids Res* 30: 325 – 327

Liu H, Zhao H, Wu L, Liu A, Zhao FJ, Xu W (2017) Heavy metal ATPase 3 (HMA3) confers cadmium hypertolerance on the cadmium/zinc hyperaccumulator sedum plumbizincicola. *New Phytol* 215: 687 – 698

Lu Z, Yu H, Xiong G, Wang J, Jiao Y, Liu G, Jing Y, Meng X, Hu X, Qian Q *et al* (2013) Genome-wide binding analysis of the transcription activator ideal plant architecture1 reveals a complex network regulating rice plant architecture. *Plant Cell* 25: 3743 – 3759

Ma X, Zhang Q, Zhu Q, Liu W, Chen Y, Qiu R, Wang B, Yang Z, Li H, Lin Y *et al* (2015) A robust CRISPR/Cas9 system for convenient, high-efficiency multiplex genome editing in monocot and dicot plants. *Mol Plant* 8: 1274 – 1284

Matsuzaki J, Kawahara Y, Izawa T (2015) Punctual transcriptional regulation by the rice circadian clock under fluctuating field conditions. *Plant Cell* 27: 633 – 648

Millar AJ, Carre IA, Strayer CA, Chua NH, Kay SA (1995) Circadian clock mutants in *Arabidopsis* identified by luciferase imaging. *Science* 267: 1161 – 1163

Munns R, Tester M (2008) Mechanisms of salinity tolerance. *Annu Rev Plant Biol* 59: 651 – 681

Murakami M, Ashikari M, Miura K, Yamashino T, Mizuno T (2003) The evolutionarily conserved OsPRR quintet: rice pseudo-response regulators implicated in circadian rhythm. *Plant Cell Physiol* 44: 1229 – 1236

Murakami M, Matsushika A, Ashikari M, Yamashino T, Mizuno T (2005) Circadian-associated rice pseudo response regulators (OsPRRs): insight into the control of flowering time. *Biosci Biotechnol Biochem* 69: 410 – 414

Murakami M, Tago Y, Yamashino T, Mizuno T (2007) Characterization of the rice circadian clock-associated pseudo-response regulators in *Arabidopsis thaliana*. *Biosci Biotechnol Biochem* 71: 1107 – 1110

Nagano AJ, Sato Y, Mihara M, Antonio BA, Motoyama R, Itoh H, Nagamura Y, Izawa T (2012) Deciphering and prediction of transcriptome dynamics under fluctuating field conditions. *Cell* 151: 1358 – 1369

Nakamichi N, Kusano M, Fukushima A, Kita M, Ito S, Yamashino T, Saito K, Sakakibara H, Mizuno T (2009) Transcript profiling of an *Arabidopsis* PSEUDO RESPONSE REGULATOR arrhythmic triple mutant reveals a role for the circadian clock in cold stress response. *Plant Cell Physiol* 50: 447 – 462

Oomen RJ, Benito B, Sentenac H, Rodriguez-Navarro A, Talon M, Very AA, Domingo C (2012) HKT2;2/1, a K^+-permeable transporter identified in a salt-tolerant rice cultivar through surveys of natural genetic polymorphism. *Plant J* 71: 750 – 762

Ouyang SQ, Liu YF, Liu P, Lei G, He SJ, Ma B, Zhang WK, Zhang JS, Chen SY (2010) Receptor-like kinase OsSIK1 improves drought and salt stress tolerance in rice (*Oryza sativa*) plants. *Plant J* 62: 316 – 329

Park YC, Lim SD, Moon JC, Jang CS (2019) A rice really interesting new gene H2-type E3 ligase, OsSIRH2-14, enhances salinity tolerance via ubiquitin/26S proteasome-mediated degradation of salt-related proteins. *Plant Cell Environ* 42: 3061 – 3076

Qi T, Wang J, Huang H, Liu B, Gao H, Liu Y, Song S, Xie D (2015) Regulation of jasmonate-induced leaf senescence by antagonism between bHLH subgroup IIIe and IIId factors in Arabidopsis. *Plant Cell* 27: 1634 – 1649

Qiao Y, Jiang W, Lee J, Park B, Choi MS, Piao R, Woo MO, Roh JH, Han L, Paek NC *et al* (2010) SPL28 encodes a clathrin-associated adaptor protein complex 1, medium subunit micro 1 (AP1M1) and is responsible for spotted leaf and early senescence in rice (*Oryza sativa*). *New Phytol.* 185: 258 – 274

Ruan SL, Ma HS, Wang SH, Fu YP, Xin Y, Liu WZ, Wang F, Tong JX, Wang SZ, Chen HZ (2011) Proteomic identification of OsCYP2, a rice cyclophilin that confers salt tolerance in rice (*Oryza sativa L*) seedlings when overexpressed. *BMC Plant Biol* 11: 34

Sakuraba Y, Jeong J, Kang MY, Kim J, Paek NC, Choi G (2014) Phytochrome-interacting transcription factors PIF4 and PIF5 induce leaf senescence in *Arabidopsis*. *Nat Commun* 5: 4636

Sakuraba Y, Bulbul S, Piao W, Choi G, Paek NC (2017) *Arabidopsis* EARLY FLOWERING3 increases salt tolerance by suppressing salt stress response pathways. *Plant J* 92: 1106 – 1120

Sanchez SE, Kay SA (2016) The plant circadian clock: from a simple timekeeper to a complex developmental manager. *CSH Perspect Biol* 8: a027748

Soni P, Kumar G, Soda N, Singla-Pareek SL, Pareek A (2013) Salt overly sensitive pathway members are influenced by diurnal rhythm in rice. *Plant Signal Behav* 8: e24738

Suzuki K, Yamaji N, Costa A, Okuma E, Kobayashi NI, Kashiwagi T, Katsuhara M, Wang C, Tanoi K, Murata Y *et al* (2016) OsHKT1;4-mediated Na^+ transport in stems contributes to Na^+ exclusion from leaf blades of rice at the reproductive growth stage upon salt stress. *BMC Plant Biol* 16: 22

Uozumi N, Kim EJ, Rubio F, Yamaguchi T, Muto S, Tsuboi A, Bakker EP, Nakamura T, Schroeder JI (2000) The *Arabidopsis* HKT1 gene homolog mediates inward Na^+ currents in xenopus laevis oocytes and Na^+ uptake in *Saccharomyces cerevisiae*. *Plant Physiol* 122: 1249 – 1259

Wang L, Fujiwara S, Somers DE (2010) PRR5 regulates phosphorylation, nuclear import and subnuclear localization of TOC1 in the *Arabidopsis* circadian clock. *EMBO J* 29: 1903 – 1915

Wang L, Kim J, Somers DE (2013) Transcriptional corepressor TOPLESS complexes with pseudoresponse regulator proteins and histone deacetylases to regulate circadian transcription. *Proc Natl Acad Sci USA* 110: 761 – 766

Wang ZY, Tobin EM (1998) Constitutive expression of the CIRCADIAN CLOCK ASSOCIATED 1 (CCA1) gene disrupts circadian rhythms and suppresses its own expression. *Cell* 93: 1207 – 1217

Wang R, Jing W, Xiao L, Jin Y, Shen L, Zhang W (2015) The rice high-affinity potassium transporter1;1 is involved in salt tolerance and regulated by an MYB-type transcription factor. *Plant Physiol* 168: 1076 – 1090

Wang Y, He Y, Su C, Zentella R, Sun TP, Wang L (2019) Nuclear localized O-fucosyltransferase SPY facilitates PRR5 proteolysis to fine-tune the pace of *Arabidopsis* circadian clock. *Mol Plant* 13: 446 – 458

Yan W, Liu H, Zhou X, Li Q, Zhang J, Lu L, Liu T, Liu H, Zhang C, Zhang Z *et al* (2013) Natural variation in Ghd7.1 plays an important role in grain yield and adaptation in rice. *Cell Res* 23: 969 – 971

Yang C, Ma B, He SJ, Xiong Q, Duan KX, Yin CC, Chen H, Lu X, Chen SY, Zhang JS (2015) MAOHUZI6/ETHYLENE INSENSITIVE3-LIKE1 and ETHYLENE INSENSITIVE3-LIKE2 regulate ethylene response of roots and coleoptiles and negatively affect salt tolerance in rice. *Plant Physiol* 169: 148 – 165

Yang Y, Guo Y (2018a) Elucidating the molecular mechanisms mediating plant salt-stress responses. *New Phytol* 217: 523 – 539

Yang Y, Guo Y (2018b) Unraveling salt stress signaling in plants. *J Integr Plant Biol* 60: 796 – 804

Zhang D, Wang Y, Shen J, Yin J, Li D, Gao Y, Xu W, Liang J (2018a) OsRACK1A, encodes a circadian clock-regulated WD40 protein, negatively affect salt tolerance in rice. *Rice* 11: 45

Zhang Y, Wang Y, Wei H, Li N, Tian W, Chong K, Wang L (2018b) Circadian evening complex represses jasmonate-induced leaf senescence in *Arabidopsis*. *Mol Plant* 11: 326 – 337

Zhou YB, Liu C, Tang DY, Yan L, Wang D, Yang YZ, Gui JS, Zhao XY, Li LG, Tang XD *et al* (2018) The receptor-like cytoplasmic kinase STRK1 phosphorylates and activates CatC, thereby regulating H_2O_2 homeostasis and improving salt tolerance in rice. *Plant Cell* 30: 1100 – 1118

Zhu JK (2016) Abiotic stress signaling and responses in plants. *Cell* 167: 313 – 324